Spring 2022

Tissue and Sex-Specific RNA Editing During Induced Acute Inflammation

Claire E. Nichols
Missouri State University, Claire306@live.missouristate.edu

Follow this and additional works at: https://bearworks.missouristate.edu/theses

Part of the Biochemistry Commons, Cell Biology Commons, and the Molecular Biology Commons

Recommended Citation

TISSUE AND SEX-SPECIFIC RNA EDITING DURING INDUCED ACUTE

INFLAMMATION

A Master's Thesis

Presented to

The Graduate College of

Missouri State University

In Partial Fulfillment

Of the Requirements for the Degree

Master of Science, Cell and Molecular Biology

By

Claire E. Nichols

May 2022

TISSUE AND SEX-SPECIFIC RNA EDITING DURING INDUCED ACUTE INFLAMMATION

Biomedical Sciences

Missouri State University, May 2022

Master of Science

Claire E. Nichols

ABSTRACT

A-to-I RNA editing is a process where select adenosine (A) nucleotides are deaminated by an editing enzyme, ADAR, to become inosines (I) in RNA transcripts. RNA editing can affect the sequence of the encoded protein and the regulation of the RNA. ADAR1 also plays a role in regulating innate immunity and its expression is upregulated during inflammation. Current data on the effects of increasing ADAR1 on RNA editing is limited, and most studies are completed only in male animals. We are interested in expanding RNA editing data to include female animals. Lipopolysaccharide (LPS) was used to induce acute inflammation and increase ADAR1. Organs were dissected four hours after LPS injection and RT-PCR was used to amplify regions around editing sites of known targets. The amplicons were sequenced and analyzed by measuring the amount of nonedited nucleotides and edited nucleotides at select sites. Inflammation did not affect levels of RNA editing in the heart or brain. There was also no significant difference in editing between males and females in the heart or brain. However, our analysis did reveal sex- and inflammation-dependent editing in the skeletal muscle. This indicates that the level of RNA editing is independently regulated in each tissue. The process by which sex-dependent editing might occur in the skeletal muscle but not in other tissues is currently unknown. Overall, this work helps us understand how the effects of infection and inflammation are regulated to minimize damage and unwanted physiological consequences.

TISSUE AND SEX-SPECIFIC RNA EDITING DURING INDUCED ACUTE

INFLAMMATION

By

Claire E. Nichols

A Master's Thesis
Submitted to the Graduate College
Of Missouri State University
In Partial Fulfillment of the Requirements
For the Degree of Master of Science, Cell and Molecular Biology

May 2022

Approved:

Randi J. Ulbricht, Ph.D., Thesis Committee Chair

Colette M. Witkowski, Ph.D., Committee Member

Joshua J. Smith, Ph.D., Committee Member

Julie Masterson, Ph.D., Dean of the Graduate College

ACKNOWLEDGEMENTS

TABLE OF CONTENTS

LIST OF TABLES

LIST OF FIGURES

INTRODUCTION

The central dogma of molecular biology describes the flow of information from the genetic material, DNA, to RNA to protein. The first step of this process is transcribing DNA into RNA. Messenger RNA (mRNA) is then decoded during translation to determine the amino acids that will be added to the protein product. During translation, ribosomal subunits bind to mRNA at an AUG initiation codon. The mRNA is pulled through the ribosome, which assists in the hydrogen binding of anticodons on tRNA molecules to the codons on the mRNA strand. Each tRNA is bound to an amino acid, so as the anticodon base pairs with the mRNA codon, the corresponding amino acid is added to the growing polypeptide chain. Once translation is complete, the mRNA, ribosome, and newly formed polypeptide dissociate from each other.

Before an mRNA transcript is translated into a protein, it undergoes several post-transcriptional processes that regulate translation of the mRNA. Some of the important processing events are polyadenylation, capping, and splicing. Polyadenylation is when 50-250 adenosine nucleotides are added to the 3' end of a transcript. These adenosine additions help protect the transcript from degradation by exonucleases and ensure that the mRNA exits the nucleus. Capping is the process of adding a 7-methylguanosine (m^7G) to the 5' end of the transcript. This cap also protects the transcript from degradation as well as recruits translation initiation factors. Splicing is a step that occurs to remove the introns of a transcript and ligate the exons of the RNA together. Specific sequences at the 5' and 3' ends of the introns as well as a branch point adenosine within the intron help to regulate where splicing occurs within the transcript. Another process that occurs before a transcript is ready for translation is RNA editing (Kumar & Mohapatra, 2021).

RNA Editing

Adenosine to inosine (A-to-I) RNA editing is a post-transcriptional process in which select adenosine nucleotides are deaminated to form inosine (Figure 1). The enzymes that perform A-to-I editing are known as adenosine deaminases acting on RNA (ADAR). ADARs bind to double stranded regions of RNA (dsRNA) in order to perform A-to-I editing. ADAR edits in a site-specific manner, binding and editing a specific adenosine nucleotide in the dsRNA region. When RNA is edited, the structure and/or function of the RNA can change. If the editing occurs within the coding region of a pre-mRNA, the amino acid sequence of the encoded protein may be altered. Editing of non-coding regions of the pre-mRNA can alter regulation, such as producing alternative splice variants, and altering the production or targeting of microRNA (miRNA).
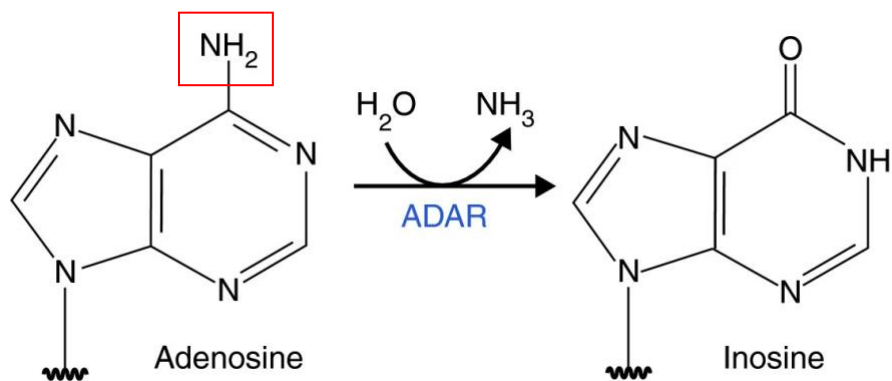
Figure 1. Deamination of Adenosine to Inosine. Hydrolytic deamination catalyzed by ADARs remove the amine group (red) from Adenosine to convert it to an Inosine. (Slotkin & Nishikura 2013).

Editing in Coding Regions. While the genomically encoded adenosine (A) base pairs with a uracil (U) nucleotide, after A-to-I editing, the new inosine base pairs with a cytosine (C) nucleotide. For this reason, during translation, inosines within a coding region of an mRNA are

"read " as guanosine by the specific tRNA that base pairs with it. This can lead to a change in the amino acid residue that is added to the growing polypeptide chain based on what is coded for by the new trinucleotide codon. For example, a genomically encoded CAG codon codes for glutamine (Q) in *Gria2* mRNA. The central A in this codon is edited so that it is recognized as CGG, thus changing the amino acid residue to arginine (R) (Kwak *et al*, 2008). The change from glutamine to arginine changes the charge at that location in the protein from negative to positive, changing the electrostatic potential. When this occurs, this specific subunit in the AMPA receptor in the brain becomes impermeable to calcium. This is necessary for normal function of the calcium channel. If this mRNA is not edited, it leads to increased calcium permeability, which causes neuronal death. The neuronal death leads to neurological phenotypes such as ALS (Rosenthal, 2015; Kwak *et al*, 2008).

RNA editing is incomplete, resulting in a portion of the RNA with inosine, while the non-edited portion is genomically encoded. The rate of editing at sites that affect the amino acid sequence is often tightly regulated. Conversely, hyperediting is a term that describes editing that occurs simply because of the existence of double stranded hairpin regions due to extensive Alu repeats in the human genome (Kim *et al*, 2004). Transcription of inverted Alu repeats will create long double stranded regions of RNA that ADAR will bind to and perform multiple A-to-I events (Rosenthal, 2015). Hyperediting is responsible for the vast majority of RNA editing events in the human genome, and often occurs in non-coding regions or pre-mRNA or in non-coding RNA.

While A-to-I editing can change the coding potential of an mRNA, this is not always the case. Changing one nucleotide of a codon may not change the amino acid due to multiple codons for the same amino acid. If editing of an adenosine nucleotide occurs in one of these locations

and does not change the amino acid coded for, the change is synonymous and there will be no change in the protein that is translated. However, regulated editing in non-coding regions of pre-mRNA, as well as editing in non-coding RNA, can affect downstream events.

Editing and RNA Splicing. A-to-I RNA editing of pre-mRNA in non-coding regions can introduce alternative splice variants by creating or eliminating important splicing elements. For splicing to occur, the 5' splice site and the intronic branchpoint adenosine (A) nucleotide bind together to form the lariat. The 5' and 3' splice sites then ligate together to form the mRNA. Without the branchpoint, splicing cannot happen. If the branchpoint is edited and resembles a G, no splicing will occur at this location. The typical splice site at the 5' end of an intron is a GU dinucleotide. If an AU dinucleotide is edited to resemble GU, this has the potential to generate a novel 5' splice site. Likewise, the typical splice site at the 3' end of an intron is an AG dinucleotide. When an intronic AA is edited to an AG dinucleotide, this can cause the introduction of a new splice site. An example of this is within the pre-mRNA that encodes the editing enzyme ADAR2. Editing in intron 4 of the ADAR2 pre-mRNA edits an AA to an AG dinucleotide, producing a new 3' splice site. This new splice site adds 47 nucleotides into the final mRNA product (Dawson *et al*, 2004). The addition of these nucleotides causes ADAR2 to become inactive, creating a negative feedback loop for ADAR2 self-regulation (Rueter *et al*, 1999).

RNA Editing and Gene Expression. Gene expression can be affected by A-to-I editing through changes in microRNA (miRNA) processing. miRNAs are small RNAs made from the introns of coding genes or from noncoding-RNAs. One role of miRNA is post-transcriptional repression of gene expression, a process called RNA interference (Nishikura, 2010). miRNAs must go through a maturation process, but once mature miRNAs are formed, they can become

involved in RNA interference and gene silencing through interactions with the RNA-induced silencing complex (RISC) (Nishikura, 2010). miRNAs are made from processing of long, imperfect double stranded precursor molecules: primary miRNA (pri-miRNA) and precursor miRNA (pre-miRNA). The pri-miRNA is transcribed as RNA that folds into a long double stranded hairpin. The pri-miRNA is cleaved by Drosha in the nucleus to form a 70-bp pre-miRNA. The pre-miRNA hairpin is then exported to the cytoplasm where it is cleaved first into a small double stranded RNA by Dicer then processed by RISC into a 22-nucleotide single stranded mature miRNA. However, because the precursors are double stranded, they may also be subject to A-to-I editing. A-to-I editing can disrupt the double stranded structure to prevent pri-miRNA processing into pre-miRNA or pre-miRNA processing into mature miRNA, downregulating the miRNA and upregulating the genes that miRNA typically silences. Moreover, since miRNA base pairs with target mRNAs to repress their expression, A-to-I editing may prevent recognition of the target and/or allow the miRNA to target a different mRNA (Kawahara *et al,* 2008). ADAR1 itself interacts with Dicer to promote the cleavage of pre-miRNA and the loading of miRNA onto RISC to silence gene expression (Ota *et al,* 2013; Zhang *et al*, 2019). Therefore, ADAR1 helps regulate gene expression through its effect on miRNA production.

ADARS

  The family of enzymes responsible for A-to-I editing are adenosine deaminases acting on RNA (ADAR). There are three ADAR enzymes in vertebrates, ADAR1, ADAR2, and ADAR3. ADAR1 and ADAR2 are active editing enzymes, while no editing activity has been identified for ADAR3 (Cho *et al,* 2003).

Protein Structure. The ADAR proteins have three main common domains (Figure 2). The deaminase domain gives ADAR its catalytic function of performing the deamination of adenosine into inosine during RNA editing (Nishikura, 2010). The deaminase domain of ADAR3 is inactive, hence its inability to perform editing (Cho *et al,* 2003). This hydrolytic deamination removes an amine group from the C6 position of adenosine, creating an inosine nucleotide (Figure 1). The deaminase domain contains three RNA contacting portions: the editing site contact residues, the 3' binding loop, and the 5' binding loop. ADAR1 and ADAR2 are similar in these regions except for the 5' binding loop, which has been characterized in ADAR2 by binding 5' to the edited site but has not yet been characterized in ADAR1. However, studies have shown that swapping the 5' binding loops in the ADAR enzymes results in no RNA editing (Matthews *et al,* 2016; Wang *et al*, 2018). This difference is one reason for the varying site selectivity and therefore different editing targets for each enzyme (Wang *et al,* 2018).

Each ADAR contains double stranded RNA (dsRNA) binding domains. ADAR1 has three dsRNA binding domains while ADAR2 only has two. These dsRNA binding domains allow ADAR to recognize and bind their targets (Herbert & Rich, 2001). All A-to-I editing occurs in regions of extended dsRNA structure. Specific adenosines will be deaminated within the double stranded region once bound by ADAR. RNA becomes double stranded through intramolecular base pairing of inverted repeats. For editing that occurs within coding regions, often one of these repeats occurs in the intron, while the other is within the exon (Jelinek & Darnell, 1972). This allows editing to remain specific to the pre-mRNA and the mRNA (where the intron has been removed) to be protected from further editing.

ADAR1 and ADAR2 also each contain a nuclear localization signal (Nishikura, 2010). This allows the major isoforms of ADAR1 and ADAR2 to primarily reside within the nucleus

(Yang *et al*, 2003). Since RNA editing occurs co-transcriptionally, it often occurs before the

mature RNA transcript is sent out of the nucleus for translation (Nishikura, 2010).
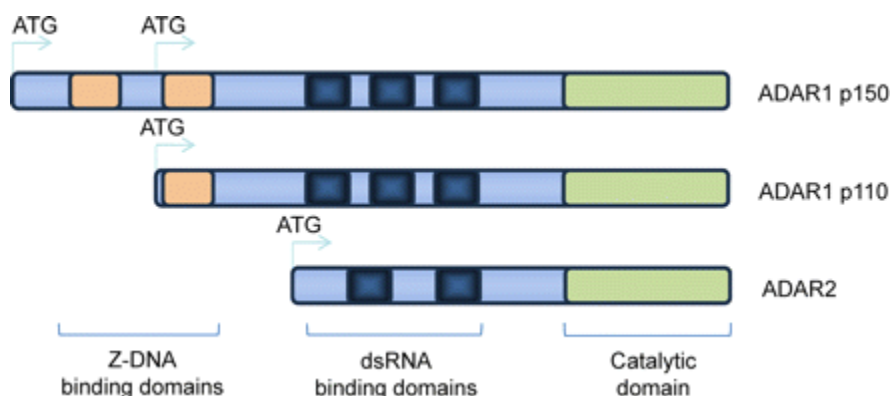
Figure 2. ADAR protein structure. ADAR1 and ADAR2 both have a catalytic domain (green) and dsRNA binding domains (dark blue). ADAR1 isoforms have three dsRNA binding domains while ADAR2 has two. ADAR1 p150 has two Z-DNA binding domains (peach), and ADAR1 p110 has only one. ADAR1 p110 is made from a start codon just upstream of Z-DNA binding domain, while ADAR p150 is made from a start codon further upstream. (Gelinas *et al*, 2011).

The ADAR1 enzyme has two different isoforms, the ~110 kilodalton ADAR1 p110 and

the longer, ~150 kilodalton, ADAR1 p150 (Nishikura, 2010). The ADAR1 p150 isoform has an

extended N-terminus that is the result of an additional exon, included by an alternative

transcription start site. The promoter that produces ADAR1 p150 will allow transcription of exon

1A, which contains an AUG start codon, so translation will start in exon 1A (George & Samuel,

1999). For ADAR1 p110, transcription produces exon 1B, which does not have an AUG start

codon, so the translation begins at the start codon in exon 2. The two start codons are in the same

frame, but the mRNA containing Exon 1A will produce 249 additional amino acids at the N-

terminus of ADAR1 p150 that are not included in the p110 isoform (George & Samuel, 1999).

Within the extended N-terminus of ADAR1 p150, there is a nuclear export signal. This allows

ADAR1 p150 to exit the nucleus and localize to the cytoplasm, giving ADAR1 p150 the ability

to participate in cytoplasmic activities related to innate immunity (Pestal *et al*, 2015; George *et al*, 2016).

There are three z-DNA binding domains in ADAR1 p150 and two z-DNA binding domains in ADAR1 p110 that are not found within ADAR2 (Figure 2). The z-DNA binding domains in ADAR1 (also called z-alpha domains) bind z-DNA as well as z-RNA. The z conformations of double stranded DNA and RNA form a left-handed helix instead of a right-handed helix found in A and B conformations of double stranded DNA and RNA. If there are mutations in the z-alpha domain, ADAR1 is not able to perform editing in the double stranded region (Nakahama *et al,* 2021), indicating that the z-alpha domains are necessary for substrate recognition and deamination of the RNA.

ADAR Activity. All ADAR enzymes nonspecifically bind to dsRNA, however, the majority of dsRNA specifically targeted by ADAR1 and ADAR2 are distinct. For example, the *CAPS1* mRNA is exclusively edited by ADAR1, while *Gria2* mRNA is exclusively edited by ADAR2 (Fu *et al*, 2016). One of the overlapping targets of editing is the mRNA for the serotonin receptor *5HT$_2$CR*. This receptor has 5 main editing sites, A, B, E, C, and D. ADAR1 is known to edit the A and B site while the E, C, and D sites are preferentially edited by ADAR2 (Costa Cruz *et al*, 2020). An interesting finding is that there is interplay between the editing enzymes at these sites. For example, at the B site, when ADAR1 is not able to edit because of a knock in mutation, there is almost no editing. But when ADAR1 can edit and there is an ADAR2 knockout, there is still a dramatic decrease in editing, indicating that both ADAR2 and ADAR1 are necessary for ADAR1 to perform its editing function (Costa Cruz *et al*, 2020).

The expression of ADAR1 p110, ADAR1 p150, and ADAR2 are different from one another. ADAR1 p110 is constitutively expressed in all tissues throughout the body. For ADAR1

p150, exon 1A transcription is induced by innate immune activation treatment with interferon, due to activation of the interferon-inducible alternative promoter (Nishikura, 2010). When inflammation is induced, the interferon response increases, therefore upregulating the ADAR1 p150 isoform. ADAR2 is expressed in most tissues throughout the body but is most highly expressed in nervous tissue and in vascular tissue (Jain *et al,* 2018).

The expression of ADAR enzymes does not necessarily mean more editing occurs. For example, when ADAR2 is present in large amounts, editing of specific ADAR2 targets does not correlate with expression of the editing enzyme, but rather correlates with the expression of the editing target (Czermak *et al*, 2018). This indicates that ADAR2 is not rate limiting. Other studies show there is dynamic regulation of editing that varies from tissue to tissue, and it does not correlate with ADAR expression (Tan *et al*, 2017). Another study showed that there was a decrease in editing of ADAR2 targets, *FLNA* and *FLNB*, in psoriasis tissue which had an increased expression of ADAR1 (Shallev *et al*, 2018). This supports the notion of competitive binding and subsequent inhibition of editing targets between ADAR1 and ADAR2. However, research on atherosclerotic tissue showed a correlation between increased ADAR1 levels and editing of the ADAR1 target Cathepsin S (Stellos *et al*, 2016). Another study used virus infection to induce inflammation and look at editing of different targets in the brain. They found no change in editing in the brain, pointing to strict regulation in this tissue even during times of inflammation (Hood *et al*, 2014). All of this taken together indicates a complex mechanism for the regulation of editing that varies between tissues and the editing target.

RNA Editing Targets

      FLNA. One editing target of the ADAR enzymes is the mRNA that encodes the filamin A protein, FLNA (Stulic & Jantsch, 2013). FLNA is an actin binding protein responsible for maintaining cytoskeletal structure and the extracellular matrix, cell-cell communication, and important signal transduction pathways (Bandaru *et al*, 2021). FLNA is made up of 24 Ig-like repeats, which consist of two light chains and two heavy chains that fold into various beta sheets and strands (Figure 3). In general, Ig-like domains are involved in processes such as cell-cell communication and signal transduction, which is why these are major functions of FLNA (Nakamura *et al,* 2007). Twenty-three of the Ig-like repeats make up 2 rods, and a 24th Ig-like repeat makes up the C-terminus of FLNA (Bandaru *et al,* 2021). The two rod sections of FLNA are bound together by two hinge regions, H1 and H2. A Ca^{2+} dependent protein, calpain, cleaves FLNA at the H2 hinge, separating Ig repeats 1-15 from Ig repeats 16-23 (Bandaru *et al*, 2021). The FLNA rod that is no longer bound to the membrane ($FLNA^{CT}$) becomes cytosolic and binds certain transcription factors in the cytoplasm, transporting them into the nucleus for gene activation (Figure 4). $FLNA^{CT}$ itself can also bind to the promoter regions of genes to promote gene activation (Bandaru *et al*, 2021).

      When the two rods are not cleaved, the protein resides on the plasma membrane, where it performs its role in cell-cell communication and cell migration (Bandaru *et al*, 2021). The cell-cell communication occurs due to the over 90 proteins with which FLNA is known to interact. Through these interactions, FLNA aids in maintaining structural integrity of cells. Alongside the structural integrity, FLNA is also found in the areas of cells responsible for helping cells to migrate, such as in the leading ends (Zhou *et al*, 2010). As cells migrate, the actin cytoskeleton

must remain intact. FLNA helps cells move by binding to and stabilizing the actin cytoskeleton. Mice that lack FLNA have developmental defects caused by the reduced movement or migration of cells. The lethal midline defects that follow this developmental abnormality include incomplete formation of the sternum and incomplete formation of the septum in the heart (Hart *et al*, 2006).
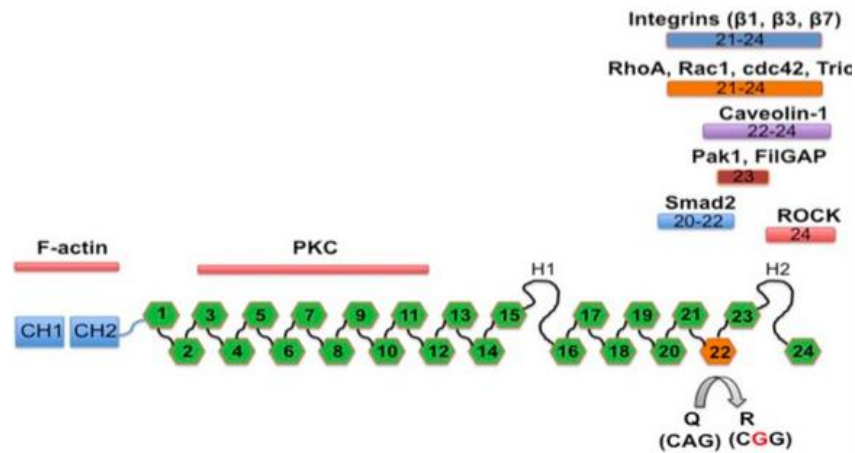
Figure 3. Structure of Filamin A protein. The filamin A protein is made of 24 Ig like repeats that are separated by two hinge regions, H1 and H2. Repeat 22 is where the edited location is, which when edited changes the CAG codon to CGG. This changes the amino acid residue from Q to R, changing the structure of the protein. Proteins that interact with filamin A at the 22nd repeat include Integrin b1, b3, and b7, RhoA, Rac1, cdc42, Caveolin-1, and Smad2. (Jain *et al*, 2018).

FLNA is expressed in all tissues throughout the body but is particularly important in the cardiovascular system (Hart *et al,* 2006; Jain *et al*, 2018). In the heart, *FLNA* is specifically found in adherens junctions, which stabilize cardiomyocytes by integrating actin filaments into the cells and anchoring them together as the heart expands throughout the cardiac cycle (Feng *et al*, 2006). Several heart diseases including aortic valve stenosis, and aortic/mitral valve regurgitation have been linked to mutations in *FLNA* (Wit *et al*, 2011). When FLNA is

11

dysfunctional, this can cause a disruption in cell-cell communication, production of extracellular

matrix, cellular stability, and important signaling pathways (Bandaru *et al*, 2021).
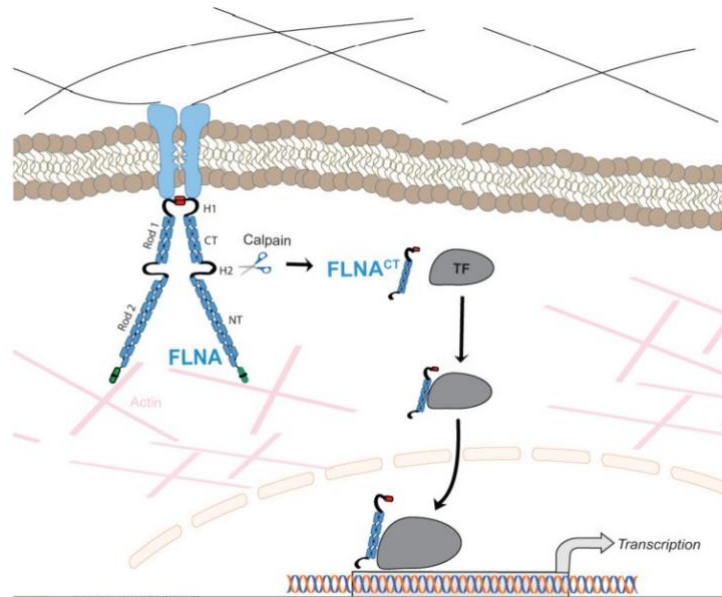
Figure 4. Schematic of FLNA homodimer cleavage by Calpain to act as chaperone for transcription factors into the nucleus. FLNA (light Blue) has two rod regions separated from the rest of the protein by hinge regions H1 and H2. Calpain, a Ca^{2+} dependent protein, will cleave FLNA at the H2 region to create a cleaved $FLNA^{CT}$. This $FLNA^{CT}$ will bind to transcription factors and act as a chaperone, bringing them to the nucleus where they will bind the promoter region and activate gene transcription. (Bandaru *et al*, 2021)

FLNA RNA Editing. FLNA is altered functionally by RNA editing. RNA editing of

FLNA mRNA causes a glutamate to arginine (Q/R) change at amino acid 2341 by exchanging an

adenosine nucleotide to an inosine nucleotide (Levanon *et al*, 2005). This alters the sequence of

the encoded protein and therefore the structure of the FLNA protein. RNA editing of *FLNA*

affects Ig-like repeat 22, which interacts with 90 other proteins (Jain *et al*, 2018). *FLNA* RNA

editing changes the electrostatic potential in this repeat, changing it from negative to positive,

which could not only alter the structure of the protein, but it could alter its interactions with other proteins (Levanon *et al,* 2005).

FLNA RNA editing is widespread throughout the body and is essential to maintaining cardiovascular health. RNA editing levels of *FLNA* are decreased in diseased cardiovascular tissues compared to healthy tissue (Jain *et al*, 2018). Eliminating editing of *FLNA* in mice leads to consequences such as mislocalization of important cell signaling molecules, increased myosin light chain phosphorylation leading to increased vascular constriction, and increased prolonged hypertension (Jain *et al,* 2018). Therefore, maintenance of *FLNA* RNA editing levels are essential for cardiac health.

ADAR2 is the primary editing enzyme responsible for editing *FLNA* mRNA. Both ADAR1 and ADAR2 are capable of binding *FLNA*, but an ADAR2 knock down eliminates most *FLNA* editing (Stulic & Jantsch, 2013). Since both ADARs can bind the site, but only one can efficiently edit the RNA, there is a potential for competitive inhibition (Riedmann *et al*, 2008). In this case, as levels of ADAR1 rise, binding of ADAR1 to the editing site of *FLNA* (but not edit the RNA) can occur at a higher rate than ADAR2, blocking ADAR2 from being able to bind and perform editing. Therefore, the overall effect of ADAR1 upregulation would be downregulation of *FLNA* RNA editing.

The gene for *FLNA* is on the X chromosome. This location is important because females have two copies of the X chromosome while males only have one. Typically, one of the X chromosomes in females undergoes inactivation. However, there are parts of the X chromosome that escape X inactivation (Medzikovic *et al*, 2020). If *FLNA* is in a part that escapes this process, expression of *FLNA* in females could potentially be higher than in males. Expression of the target plays an important role in regulating the amount of editing, where the rate of editing

decreases with amount of target expression (Czermak *et al,* 2018). Therefore, if there is a gene dosage effect and *FLNA* is expressed more in females, one could expect a lower percent editing overall in females compared to males.

FLNA in the Heart. One of the important functions of FLNA in the heart involves its participation in cell signaling pathways such as the RhoA/ROCK and PLC/PKC pathway (Figure 5). FLNA participates in this pathway by interacting with RhoA and ROCK (Nakamura *et al,* 2011; Loirand *et al,* 2006). If *FLNA* editing is disrupted, then the cell signaling pathway between Ras homolog family member A (RhoA)/ Rho associated coiled-coil containing protein kinase (ROCK) and phospholipase C (PLC)/ protein kinase C (PKC) is disrupted. This pathway is important for maintaining the structure of the vascular smooth muscle cells (Jain *et al,* 2018). When this pathway is disrupted through elimination of *FLNA* editing, cardiac remodeling is observed in areas where there are vascular smooth cells such as the blood vessels entering and leaving the heart (Jain *et al,* 2018). This remodeling leads to increased work on the heart because it is having to overcome a greater resistance in these blood vessels. The increased strain on the heart leads to cardiomyocyte hypertrophy resulting in systemic hypertension. Prolonged systemic hypertension increases the risk of subsequent heart failure (Figure 6). In order to maintain normal physiology in the heart, there must be a normal level of *FLNA* mRNA editing (Jain *et al,* 2018). It is worth noting that these studies were performed in mice where RNA editing was permanently disrupted, from birth. We do not know the consequences of temporary alterations to *FLNA* RNA editing but predict that reduction of *FLNA* editing for a short time may increase blood pressure and the work of the heart. However, we would assume this would return to normal as the editing of *FLNA* resumes.
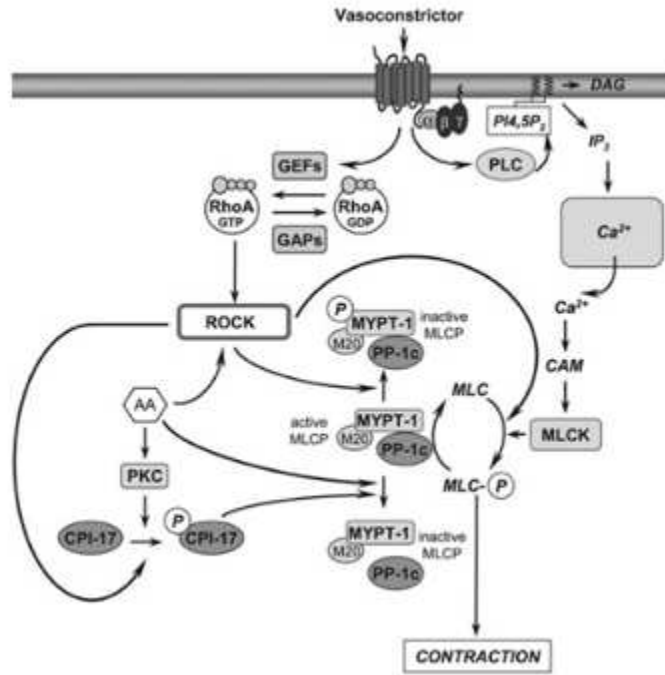
Figure 5. RhoA/ROCK pathway leading to vascular smooth muscle cell contraction. When activated, RhoA will activate ROCK which can either phosphorylate CPI-17 to cause inactive MLCP, or it will directly inactivate MLCP. Inactivating MLCP increases the phosphorylation of myosin light chain, which causes smooth muscle cell contraction (Loirand *et al*, 2006).

FLNB. The Filamin-B protein (FLNB) has the same protein structure as FLNA and is edited by ADAR2 at the same position as FLNA, resulting in a similar Q to R change. The *FLNB* gene is on chromosome 3 in humans and chromosome 14 in mice and is ubiquitously expressed (Sheen *et al*, 2002) but plays an important role in joints and skeletal development (Zhou *et al*, 2007). *FLNB* editing is highest in the musculoskeletal system, which differs from *FLNA*, which has the highest percentage of editing in nervous and cardiovascular tissues (Czermak *et al*, 2018). There has been little research on *FLNB* editing, but since it is edited at the same location as *FLNA*, it is thought that decreased editing has similar consequences in protein-protein interaction and extracellular matrix integrity. Some studies have also shown changes in *FLNB* editing in cancers such as human hepatocellular carcinomas (Chan *et al,* 2014). This change in

physiology is likely to have the most consequences in the places *FLNB* is most highly expressed, such as skeletal muscle.
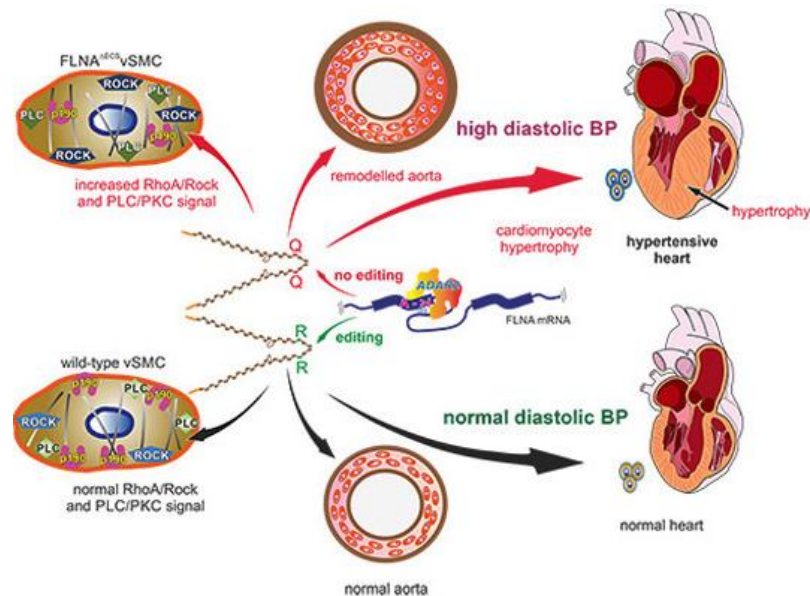
Figure 6. Effects of RNA editing in cardiovascular tissue. When edited, *FLNA* localizes RhoA/Rock and PLC/PKC signals to the cell membrane, causing normal vascular smooth muscle cell (vSMC) contraction and normal structure of cardiovascular tissue. When there is no editing of *FLNA*, there is mislocalization of RhoA/Rock and PLC/PKC signals, causing increased contractility, vascular remodeling, increased diastolic blood pressure, and cardiomyocyte hypertrophy (Jain *et al,* 2018).

CAPS1. The RNA encoding calcium activator protein for secretion 1 (CAPS1) is edited by ADAR1. CAPS1 promotes regulated exocytosis of dense core vesicles and small clear synaptic vesicles (Miyake *et al*, 2016). This function is important in regulating proper neurotransmission as well as general secretion in other tissues. *CAPS1* is edited in its c-terminal domain, the site where it interacts with SNARE proteins to create the SNARE complex for secretion. Its editing results in an amino acid change from glutamate to glycine. When *CAPS1* is edited, the novel protein has more efficient vesicle secretion than when the protein remains unedited (Miyake *et al*, 2016; Ulbricht *et al*, 2017; Shumate *et al,* 2021). *CAPS1* RNA editing is

seen in multiple different tissues such as the heart and brain, with the highest editing seen in the hippocampus, cerebellum, and frontal cortex (Ulbricht *et al*, 2017). Since *CAPS1* is edited by ADAR1, it is important to observe the editing of this target during inflammation, due to the role of ADAR1 p150 in regulating innate immunity.

Inflammation

Inflammation is a tightly regulated process that responds to any pathogen, infection, or foreign substrate in the body. Inflammation is typically resolved in a short period of time. The initial line of defense with inflammation is the innate immune system. Signaling molecules from the innate immune system, called cytokines, travel throughout the body, alerting cells and tissues to prepare for pathogens. The main inflammatory cytokines are interleukin-6 (IL-6), signal transducer and activator of transcription 1 (STAT-1), tumor necrosis factor alpha (TNF-α), and interferon beta (IFN-β). These cytokines cause a cascade of events that alter gene expression and attract immune cells responsible for inflammation, such as macrophages, dendritic cells, neutrophils, and natural killer cells to the site of infection or pathogen (Zhang & An, 2007).

The innate immune response is in place to escalate the response to pathogens quickly and to rid the body of them. If the pathogen is not eliminated, the innate immune response transitions into adaptive immunity, the long-term process for handling inflammation. The adaptive immune system is composed of immune cells such as B-cells and T-cells. These immune cells help create antibodies, a type of memory cell that allows the body to recognize a pathogen that has previously attacked. Having antibodies helps to fight the same infection in a shorter amount of time during future infections. If the adaptive immune response is not activated and the innate

immune response is unregulated, there are severe consequences to the prolonged inflammation that follows (Bachmann & Kopf, 2001).

ADAR1 and Inflammation. Since ADAR1 p150 is interferon inducible, its transcription is upregulated during times of inflammation when type 1 interferons are produced, also known as the interferon response. The interferon response helps alert neighboring cells of the pathogen causing the inflammation. When the interferon response is activated, there is an increased production of interferon beta (IFN-β), which binds the interferon alpha and beta receptors on neighboring cells. IFN-β binding to these receptors causes the phosphorylating janus kinase (JAK) protein at the receptor to cross phosphorylate the STAT1 and STAT2 proteins that are recruited to this receptor. Phosphorylation of the STAT proteins activates nuclear factor kappa-light-chain-enhancer of activated B cells (NFκB) (Seif *et al*, 2017). NFκB is a transcription factor that induces transcription of interferon stimulated genes (ISG's), including ADAR1 p150. Following an increase in interferon response due to inflammation, there will be an increased amount of ADAR1 p150 from its interferon inducible promoter (George & Samuel, 1999).

While ADAR1 p150 is transcribed from a promoter that is targeted by innate immune activation, ADAR1 p150 also has an important role in regulating the innate immune response. Mice deficient in ADAR1 have increased inflammatory responses in hepatocytes due to increased pro-inflammatory cytokine levels and upregulation of NFκB (Ben-Shoshan *et al*, 2017). Overexpression of ADAR1 leads to decreased production of inflammatory cytokines, but deletion or knock down of ADAR1 results in increased inflammation and tissue damage, further supporting the role of ADAR1 in inflammation suppression (Liu *et al*, 2018). Moreover, reintroducing ADAR1 after increased production of pro-inflammatory cytokines results in a return back to normal cytokine levels (Wang *et al*, 2015). ADAR1 suppression of the innate

immune response is an imperative regulator of innate immunity. Mice that do not express ADAR1 p150, while still expressing ADAR1 p110, die before birth (Hartner *et al,* 2009). However, mice that do not express ADAR1 p150 and also have a deletion of the melanoma differentiation-associated gene 5 (MDA5) dsRNA receptor will live to full term (Liddicoat *et al*, 2015). MDA5 is a dsRNA sensor whose role is to sense exogenous dsRNA and activate the mitochondrial antiviral-signaling protein (MAVS), which in turn activates downstream signals that upregulate pro-inflammatory cytokines. ADAR1 p150 inhibits MDA5 from sensing endogenous dsRNA via RNA editing, which destabilizes the mRNA, causing it to be single stranded and no longer sensed by MDA5. If MDA5 senses endogenous dsRNA, this results in upregulation of the innate immune response in the absence of a pathogen, leading to autoimmune diseases. The role ADAR1 p150 induction plays in suppressing innate immunity through the MDA5 receptor is essential for survival.

Consequences of Inflammation. The innate immune system is activated in the presence of a virus, toxin, bacteria, or anything the body does not recognize as itself. This is useful to quickly destroy a foreign entity. However, if the innate immune response is not regulated, it can lead to an over-response of inflammation which in turn can lead to tissue damage and/or disease.

Myocarditis is a general inflammation of the heart that is caused by activation of innate immunity through stress, disease, and either bacterial and/or viral infections. Myocarditis is associated with cardiomyocyte hypertrophy, increased fibrosis leading to decreased contractility, and more work needed for the heart to function properly. While myocarditis can resolve with treatment from anti-inflammatory drugs, if unchecked it can eventually lead to heart disease and eventual heart failure. Often, the symptoms of acute myocarditis go unnoticed in individuals, leading to sudden death in seemingly healthy people (Cooper, 2009).

Autoimmune diseases occur when the body recognizes part of itself as foreign. Examples of autoimmune diseases are things such as rheumatoid arthritis, psoriasis, and Aicardi-Goutieres syndrome (AGS). In all of these autoimmune diseases, there is uncontrolled inflammation in some part of the body, leading to abnormal physiology. In AGS, there is inflammation in the brain causing severe swelling. This swelling leads to symptoms like body stiffness, headaches, blurred vision, and seizures (Rice *et al*, 2007). One of the mutations that causes AGS is found in the ADAR1 gene. This mutation leads to downregulation of RNA editing. If ADAR1 is not able to edit dsRNA, it will not be able to inhibit MDA5 from recognizing endogenous dsRNA, thus MDA5 will upregulate inflammatory cytokines without the presence of a foreign pathogen (Guo *et al*, 2021). The unregulated innate immune response causes the brain to swell and causes the symptoms associated with AGS. This autoimmune disease is lethal from a young age, with most patients not living past childhood (Rice *et al,* 2007).

Sex Differences in Inflammation. While there are many pathways involved in inflammation, one specific pathway goes through a toll-like receptor (TLR), TLR4. TLRs are transmembrane pattern recognition receptors (PRRs). There are several TLRs in humans, with TLR4 being one that upregulates inflammation in response to certain sequences found on gram-negative bacteria, known as pathogen associated molecular patterns (PAMPs). When TLR4 is activated by binding to a PAMP, it recruits proteins that upregulate NFκB, and therefore upregulate the transcription of inflammatory cytokines and ISGs.

One reagent commonly used in research that triggers the innate immune system via TLR4 is lipopolysaccharide (LPS). LPS is an endotoxin found on the surface of gram-negative bacteria, and it contains a PAMP recognized by TLR4. TLR4 on macrophages can recognize LPS, but it requires the co-receptor CD14, as well as the LPS binding protein (LPB), in order to cause the

activation of TLR4. When this occurs, TLR4 recruits the protein MyD88, which causes a cascade of events leading to the activation of NFκB, which transcribes many pro-inflammatory cytokines (Akira, 2004).

As stated earlier, myocarditis is an inflammatory response in the heart. Viruses, such as Coxsackievirus B3 (CVB3), can induce this inflammation through the TLR4 pathway. TLR4 causes the downstream effect of upregulated inflammatory cytokines including IL-10 and ADAR1 p150. During inflammation, TLR4 has increased expression on macrophages and mast cells in male mice compared to females (Marriott *et al*, 2006; Frisancho-Kiss *et al,* 2007). Because of this, male mice have increased expression of genes that lead to myocarditis. To determine if the male sex hormone, testosterone, plays a role in myocarditis severity, female mice and male mice were treated with testosterone during CVB3 infection. Testosterone treatment increased myocarditis and myocardial fibrosis in males but not females (Cavasin *et al,* 2006). On the other hand, male mice subjected to hemorrhagic trauma had lower levels of TLR4 after estrogen treatment compared to male mice that did not have estrogen treatment (Hsieh *et al*, 2007), indicating the protective effect of estrogen in relation to TLR4 activation.

When a pathogen infects a tissue, the immune reaction that occurs triggers the release of cytokines from immune cells infiltrating the affected tissue. T-helper cells type 1 (Th1) or T-helper cells type 2 (Th2) are T cells that secrete different cytokines when activated. The Th1 cells secrete cytokines such as IFN-γ, which is a pro-inflammatory cytokine that activates NFκB. Th1 cells can be activated by testosterone, which is why males tend to have a Th1 response and increased levels of inflammation (Spellberg & Edwards, 2001). Th2 cells secrete cytokines such as IL-10, which is an anti-inflammatory cytokine. Th2 cells can be activated by estrogen, which is why females have an overall anti-inflammatory response and have decreased levels of

myocarditis during inflammation (Spellberg & Edwards, 2001). Th2 cells in females also have significantly more TLR4 on their surface, causing a robust response to pathogens due to their increased ability to detect infection (Scotland *et al*, 2011). The higher level of TLR4 along with the production of anti-inflammatory cytokines creates an overall strong response to pathogens with a regulated response to the inflammation.

ADAR1 p150 is an anti-inflammatory cytokine that is upregulated by TLR4 activation (Zhang *et al*, 2019). Studies have shown that factors downregulated by ADAR1 p150, such as MAVS and MDA5, are increased during inflammation in the heart, and significantly different between males and females (Koenig *et al,* 2014). To our knowledge, the current literature has only examined the editing activity of ADAR1 in male mice. Since the factors linked to ADAR1 p150 are sex-dependent, it is possible that ADAR1 p150 activity is also sex-dependent. We will induce inflammation and ADAR1 p150 in both male and female mice using LPS. Similar to CVB3, LPS will induce inflammation through the TLR4 pathway, upregulating NFκB, which upregulates inflammatory cytokines, including ADAR1 p150. We are specifically interested in innate immune activation of the heart, due partially to its link to myocarditis, but also due to the RNA editing targets expressed there.

The majority of RNA editing data has been collected in the brain, since the majority of re-coding RNA editing targets have been shown to be involved in neurotransmission (Rosenthal, 2015). While it is clear that RNA editing is tissue-specific, it is unclear how this editing is regulated (Tan *et al*, 2017; Shallev *et al,* 2018; Stellos *et al,* 2016). The literature currently has no information on whether RNA editing is sex-dependent, and studies are performed almost exclusively in male mice. To our knowledge, no studies have been published comparing editing between males and females. Moreover, while some studies analyzed RNA editing levels during

inflammation (Stellos *et al,* 2016; Hood *et al,* 2014; Shallev *et al*, 2018)., we do not know if inflammation or other genetic conditions that induce ADAR1 p150 could differentially affect the amount of editing at re-coding sites based on the sex of the organism. The lack of information on sex-dependent RNA editing, and the lack of clarity on ADAR1 p150 induction of editing will be addressed by this thesis. Here we will fill a gap in knowledge by providing a profile of RNA editing in male and female mice, in the heart, brain, and skeletal muscle, and with and without acute inflammation, ultimately determining if RNA editing is sex-specific, tissue-specific and/or inflammation-specific.

Investigating the Tissue and Sex-Specific RNA Editing

Induction of ADAR1 p150 plays an important role in quenching the innate immune response in the cytoplasm of the cell, but it is also possible that upregulating the amount of ADAR1 available in the cell changes its RNA editing activity (Stellos *et al,* 2016; Shallev *et al*, 2018; Hood *et al*, 2014). One study showed that global inflammation due to activation of the innate immune response did not affect RNA editing in the brain for several targets, indicating that levels of ADAR do not correlate with the amount of editing that occurs (Hood *et al*, 2014). Another study profiled the editing of *FLNB* throughout the body and found that in all tissues, the level of editing did not correlate with the expression of ADAR (Czermak *et al*, 2018). However, one study did show that changes in the levels of ADAR1 in atherosclerotic tissue did affect RNA editing levels of an ADAR1 target (Stellos *et al*, 2016). These two opposing findings have led us to believe that regulation of RNA editing is complex and dependent upon more than just the amount of ADAR present. We believe that the tissue where editing is occurring might be an

important factor that regulates ADAR activity. Moreover, it is also possible that the sex of the organism plays a role in the editing level.

The goal of this research is to determine if inflammation alters RNA editing in a tissue specific and/or sex-specific manner. To do this, ADAR1 p150 will be upregulated through LPS induced inflammation, and RNA editing levels in heart, brain, and skeletal muscle will be quantified. In preliminary data, *CAPS1* RNA editing was significantly increased in the heart during a viral infection that triggered ADAR1 p150 upregulation in mice (Figure 7). Despite wide-spread induction of ADAR1 p150, changes in *CAPS1* editing were only seen from heart tissue, while the level of editing in the brain remained unchanged. This indicates a difference in the regulatory mechanism for editing in the individual tissue. If ADAR1 p150 induction positively affects RNA editing of ADAR1 targets like *CAPS1*, we may also expect that upregulation of ADAR1 may decrease editing of ADAR2 mRNA targets due to competitive inhibition. Therefore, we expect editing levels of ADAR2 targets, such as *FLNA* and *FLNB*, to be reduced in the heart during inflammation.

We will quantify RNA editing levels of *CAPS1*, *FLNA*, *FLNB*, and *Gria2* in the brain. Based on previous studies, we expect no changes in *CAPS1* editing in LPS treated mice. The same study that saw no interferon-induced changes in *CAPS1* mRNA editing in the brain, also saw no changes in *FLNA* editing in the brain (Hood *et al*, 2014), therefore, we expect that LPS will not affect *FLNA* in the brain. *FLNB* is similar to *FLNA* in structure and function, and it is also edited in the same location as *FLNA*. We expect that it too will not be affected by LPS. We are interested in the editing of *Gria2* because this ADAR2 target is expressed exclusively in the brain and must have 100% editing for calcium permeability in neuron channels (Rosenthal 2015), which is essential. We wanted to ensure that an increase in ADAR1 was not also causing

a decrease in *Gria2* editing due to competitive inhibition of ADAR2, and thereby destroying healthy neurons.

We will also examine RNA editing of *CAPS1*, *FLNA*, and *FLNB* in the heart. We will continue to look at *CAPS1* to see if the tissue specific editing changes seen in the heart during viral infection also occurs during LPS treatment, an entirely different mode of inflammatory activation. *FLNA* is an important target because of the known physiological consequences in the heart when editing of this target is decreased, such as hypertension, cardiomyocyte hypertrophy, and eventual heart failure (Jain *et al*, 2018). The expression of *FLNB* in the heart is not as high as that of *FLNA*, but because of the similarities, it is a good target to look at RNA editing in the heart.
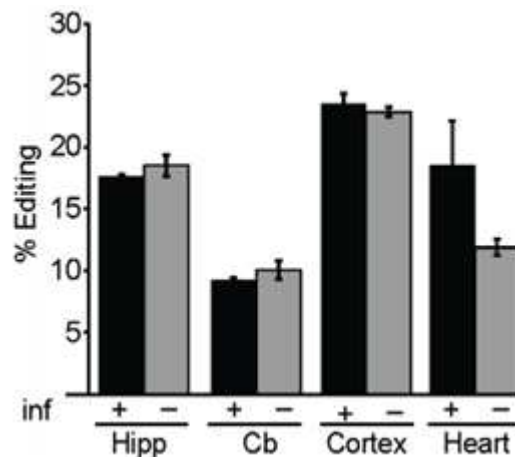
Figure 7. Preliminary data quantifying *CAPS1* RNA editing after viral infection. *CAPS1* RNA editing quantified by next generation sequencing from mouse heart and brain in uninfected mice and mice infected with a Reovirus. (Ulbricht, unpublished).

Quantifying RNA Editing in RT-PCR Products of *FLNA*, *FLNB*, *CAPS1*, and *Gria2* from Heart and Brain Tissues of Mice

We quantified RNA editing by sequencing RT-PCR products of *FLNA*, *FLNB*, *CAPS1* and *Gria2*. Wild-type C57/Bl6 mice were injected with either LPS or saline, and four hours after injection, the organs were harvested and snap frozen in liquid nitrogen. RNA was isolated, converted to cDNA, then PCR performed. PCR amplicons were sequenced to determine the rate of editing in each of these targets. The amount of G nucleotides versus the amount of A nucleotides detected at the edited location will be used to quantify the rate of editing. RNA editing is not complete, meaning some sequencing results will have an A nucleotide while others will be edited and have a G nucleotide. It is expected that *FLNA* and *FLNB* from mice who received LPS injections will have lower editing levels in the heart compared to the editing levels in the heart of mice injected with saline. The opposite is expected for *CAPS1* editing. We expect the RNA editing levels from the brain of all three targets to be similar in LPS and saline injected mice. We also expect editing of *Gria2* to remain the same between treatment groups.

Quantifying RNA Editing in RT-PCR Products of *FLNA* and *FLNB* from Skeletal Muscle of Mice

Next, *FLNA* and *FLNB* RNA editing will be quantified in skeletal muscle from inflamed and normal mice. FLNA plays a vital role in the proper physiological processes of the heart while FLNB plays a major role in processes of the musculoskeletal system. When FLNB is knocked out in mice, they have decreased amounts of hyaline cartilage, vertebral and joint malformations, as well as general skeletal development abnormalities (Zhou *et al,* 2007). While FLNA and FLNB have similar structure and function, their major roles take place in varying

locations of the body. They also have varying locations for RNA editing levels. While *FLNA* has highest editing levels in nervous and cardiovascular tissues, *FLNB* shows highest editing levels in the musculoskeletal system as well as the heart (Czermak *et al,* 2018). Skeletal muscle is also an important tissue that responds to inflammation. After quantifying editing changes in the heart and brain for *FLNA* and *FLNB*, observing editing of these same targets in skeletal muscle will give a broader view of how editing might be changing globally during inflammation rather than only in two specific tissues. This will be done similar to the methods described for first aim, but from cryopreserved skeletal muscle isolated from the abdominal wall of the same mice.

If we were to see editing changes in skeletal muscle and heart but not the brain, this could indicate that RNA editing in the brain is more tightly regulated than other tissues, or that there is a different regulatory mechanism for each tissue in the body. Furthermore, analysis of RNA editing levels of the same targets in tissues where they play both minor and major roles may allow us to uncover special mRNA-specific regulatory events.

Overall, a more complete picture about how RNA editing is affected by innate immunity may help us to understand some of the consequences of innate immune activation in auto-immune disease and long-term infection, versus shorter stents of activation such as soft-tissue trauma and short-term infection. These results could also lead to a better understanding of how global inflammation affects individual organs as well as the different responses to inflammation seen in males and females. By understanding this on a deeper level, symptoms of inflammation could be treated more specifically for each sex and organ rather than trying to treat the inflammation as a whole.

MATERIALS AND METHODS

The research performed for this project used tissues from mice that were previously injected and dissected. The injection and dissection protocol is outlined for future replication, but all the research I performed was on post-mortem tissue samples. Therefore, IACUC approval was not required for this project. I was assured that ethical research practices were followed in obtaining the tissue samples that I received.

LPS and Saline Injections

Intraperitoneal injection of lipopolysaccharide (LPS) was used to trigger acute inflammation in mice. Pairs (experimental and control) of age-matched, litter-mate mice were co-housed after weaning. Once the co-housed pairs were between 8 and 13 weeks of age, each pair was injected with either LPS (experimental) or saline (control). The LPS (Sigma Aldrich L2630 - 25 mg) was suspended in 25 mL of saline to reach the final concentration of 1 mg/mL. For the injections, the mice were first weighed individually. The mice were held in a supine position and given an intraperitoneal injection in the lower right quadrant of the abdomen with 15 mg/kg body weight of 1 mg/mL LPS or an equal volume of saline. All animal work was performed by other graduate students in the lab, and Missouri State University IACUC approval was not required for my work with the tissues post-mortem.

Dissection and Cryopreservation of Tissue

Four hours after saline or LPS injection, the mice were euthanized and dissected. The mice were taken out of their cage and a mixture of isofluorene and oxygen was used to

anesthetize them. The mice were then cervically dislocated and decapitated. The brain, right eye and pituitary gland were isolated from the head. The heart, left kidney, and pancreas were harvested from the body. Skeletal muscle forming the upper left abdominal wall was also isolated from the mice. The harvested organs were immediately placed in liquid nitrogen and stored in -80 ºC.

Homogenizing Tissue

In order to isolate RNA, whole organs were homogenized in Ambion TRIzol reagent (catalog #15596018). The organs were removed from storage at -80 ºC and placed on dry ice. The organs were weighed, then placed in 15 mL conical tubes on wet ice. The protocol called for 1 mL of cold TRIzol per 100 mg of tissue, however, 1/10th of this was added and the suspensions placed on ice. The largest weighing organ was used as the standard for the amount of TRIzol for the rest of the organs being homogenized at one time. A FisherBrand Ultrasonic Liquid Processor (model #FB-120) was used to disrupt the tissue. For each whole organ, 20 seconds of sonication was performed 2-3 times. Between each round of sonication, the suspension was left on ice for approximately 30 seconds. The sonicator was kept on 60% power during each sonication. Homogenates were either immediately processed to isolate RNA or stored at -80 ºC for future use. Fresh homogenates worked best, however, frozen homogenates were often used due to time constraints.

RNA Isolation

To isolate RNA, homogenized tissue was thawed on ice. Then 900 μL of TRIzol was added to 100 μL of homogenate. Two hundred microliters of chloroform was added to the

mixture and the samples were vortexed. After vortexing, the samples were centrifuged at 13,000 x g for 5 minutes. A p1000 micropipette was outfitted with a p1000 tip then a p200 tip and the aqueous layer (on top) was carefully removed and transferred to a new 1.5 mL tube. The organic layer and interface were saved at -80 ºC for future isolation of protein or genomic DNA, if necessary. An equal volume of isopropanol was added to the aqueous layer and together they were spun for 10 minutes at 13,000 x g to pellet the RNA. The 1.5 mL tubes were spun with the hinges facing out so the pellet will be present on the same side of the tube as the hinge. Then the pellet was washed with 500 μL of 75% ethanol and centrifuged for 5 minutes. The ethanol was decanted, and the tubes were left upside down to dry until the RNA pellet was completely dry, about 10-15 minutes. The pellet was resuspended in diethyl pyrocarbonate (DepC) treated nuclease free water and placed at -20 ºC until completely frozen to prepare for quantification.

RNA Quantification

The RNA was thawed at room temperature and vortexed thoroughly. The same DepC treated nuclease free water used to resuspend the pelleted RNA was used as the blank on the IMPLEN nanophotometer NP80. One microliter of the water was placed on the nanophotometer and blanked. The absorbance of the water was then measured to make sure the blank worked accurately, meaning the nanophotometer measured a concentration of 0 ng/μL. If the nanophotometer did not give us a concentration of 0 ng/μL, then the same water was used to re blank the machine. Then the RNA was vortexed and 1 μL of the sample was placed on the nanophotometer to measure the concentration in ng/μL. The concentration of RNA in ng/μL was recorded, along with the A_{260}, and the A_{260}/A_{280} ratio. Once quantified, the RNA was either used immediately for RT-PCR or was stored at -80 ºC.

RT-PCR

To amplify edited sites on target mRNAs, first, complementary DNA (cDNA) was made by reverse transcription. One microgram of RNA was added into a 20 μL reverse transcription reaction using the Applied Biosystems High Capacity cDNA Reverse Transcription Kit (catalog #4368814). Two master mixes were made. Each master mix contained random primers, buffer, deoxynucleotides (dNTPs) and water. However, one had reverse transcriptase (RT) and the other had no RT (water instead). The master mix was aliquoted into PCR tubes. Each reaction contained 1X random primers, 1X reverse transcription buffer, 0.5X dNTPs and 1 μL RT (or water). The samples were run on the thermocycler under the HC_RT protocol (Table 1).

Table 1. Cycling conditions for reverse transcription

Step	Temperature	Time
1.	24 ºC	10:00
2.	37 ºC	1:00:00
3.	85 ºC	10:00
4.	4 ºC	Infinite Hold

Once the cDNA was made through reverse transcription, polymerase chain reaction (PCR) was performed to amplify the region surrounding the editing site on each target. A PCR master mix containing a forward and reverse primer, as well as a polymerase mix that contains buffer, dNTPS and the Taq Polymers was made. The master mix was aliquoted into PCR tubes with cDNA. Each reaction was 50 μL and contained 25 μL of ThermoScientific 2X DreamTaq polymerase master mix (catalog #K1081), 2 μL of 200 ng/μL forward and reverse primer, 16 μL

of DepC water, and 5 μL of cDNA. The no RT cDNA was used as a negative control. An additional negative control was used that did not contain cDNA. The reactions were then placed in the thermocycler and the protocol containing the proper melting temperature for the target of interest was chosen (Table 2). The specific forward and reverse primers for the target gene of interest are listed in Table 3 and Table 4.

Table 2. Cycling conditions for editing targets

Step	Temperature	Time
1	95 ºC	5 min
2	95 ºC	30 s
3	60 ºC (FLNA), 56 ºC (FLNB), or 54 ºC (CAPS1)	30 s
4	72 ºC	30 s
	GO TO step 2, 35x	
5	72 ºC	10 min
6	12 ºC	Hold

Gel Electrophoresis

Agarose gel electrophoresis was used as a verification step to make sure the PCR correctly amplified the product of interest. Either a 1%, 1.5%, or 2% agarose in 1 X sodium borate (SB) buffer was melted in a microwave, then 8×10^{-4} mg/mL of ethidium bromide was added to the melted gel, mixed and poured into a gel molding tray. After solidification, the electrophoresis chamber was filled with 1 X SB, then 5 μL of PCR product was loaded into each well. Three microliters of the ThermoScientific GeneRuler 1kb Plus DNA Ladder (0.1 μg/μL)

was loaded into at least one well of each gel. Samples were electrophoresed at 250 V for 25-30 minutes. The gel was visualized using UV light on a BioRad GelDoc Go Imaging System (model Ver. A 12012149). Products were verified by the presence of a band of the desired size in the +RT samples (Table 3), and no band in the -RT samples and/or the no template reaction. Verified +RT amplicons were purified by one of two different methods: gel purification or column purification. Column purification was used if the only product seen in the +RT sample represented that of the desired product. Gel purification was used if non-specific products were also present.

Table 3. PCR primers

Target	Sense (S) or Antisense (AS)	oRU #	Sequence	Product Length (bp)
FLNA	S	101	CTGATAGCCCCTTCGTGGTG	249
	AS	102	AGATGCCATTCTCTCGTGGG	
FLNB	S	116	GAGTTCAGCATCTGGACCCG	330
	AS	84	CCCTTTCGCACCATTCAACC	
CAPS1	S	48	AATGATCACACTTTTGGTGGCAAAGTTG	506
	AS	49	CTGTCCTTCATGCTGATACCTTGTAAG	

Gel Purification

To purify DNA for future sequencing, the entire remaining PCR product was loaded into one well of an agarose gel. This gel was electrophoresed the same way as in the verification step. The gel was viewed using a short wave transilluminator. Bands were excised from the gel using a razor blade. The gel slice was placed in a 1.5 mL centrifuge tube and the samples were

weighed. DNA was purified from the gel slice using the Promega Wizard® SV Gel and PCR

Purification kit (catalog # A9282). An equal volume of membrane binding solution was added to

each gel slice (0.206 g = 206 µL of membrane binding solution). Each tube was vortexed and

placed in a heating block at 65 ºC until the gel slice was completely melted. The melted solution

was vortexed again then added to a labeled minicolumn. The minicolumn was centrifuged at

13,000 x g for one minute, then the flowthrough was decanted. Then 700 µL of membrane wash

solution was added to the minicolumn and centrifuged again for one minute. Next, 500 µL of the

membrane wash solution was added to the column and the column centrifuged for 5 minutes at

13,000 x g. The flowthrough was discarded and the minicolumn centrifuged for one more minute

to dry. The mincolumn was transferred to a new 1.5 mL centrifuge tube. Finally, 30 µL of heated

(~ 95 ºC) nuclease free water was added to the minicolumn and incubated at room temperature

for one minute. The minicolumn was centrifuged for one minute at 13,000 x g to elute the DNA.

Once all the DNA samples were eluted, a nanophotometer was used to quantify the DNA

concentration.

Column Purification

To purify DNA via column purification, an equal volume of membrane binding solution

is added to the remaining PCR product, which is immediately added to a minicolumn from the

Promega Wizard® SV Gel and PCR Purification kit (catalog # A9282). The rest of this protocol

is the same as performed for the gel purification, starting after the gel has been completely

melted.

NGS/Sanger Sequencing

To quantify the occurrence of RNA editing, samples were sent to GeneWiz for either next generation sequencing (NGS) or Sanger sequencing. Our *FLNA* samples were sent for Sanger sequencing, but *FLNB* and *CAPS1* did not produce as clean of a chromatogram, so those samples were sent for NGS. For pre-mixed Sanger sequencing, 1 ng/μL of DNA is sent with a total mass of 10 ng. Five microliters of a specific primer (Table 3) that has been diluted to 5 μM is added to make the reaction a total of 15 μL. To analyze the Sanger sequencing chromatograms, the online software ImageJ was used to measure the difference in the area under the peaks for each nucleotide at the edited site. Once the areas of each peak are calculated, they are compared using the equation: percent G = [G/(G+A)] x 100, where G is the area under the peak for G nucleotides and A is the area under the peak for A nucleotides (Shi Y *et al*, 2017). The resulting answer is the percent of G nucleotides, which is the same as the percent editing.

For NGS, between 100 - 500 ng of DNA was sent to Genewiz for Amplicon EZ sequencing. For this sequencing, the product must be less than 300 bp long. For NGS, we multiplexed our reactions to increase throughput. The sense primer is labeled with one of 6 unique barcodes of 5 nucleotides (Table 4). Once PCR is performed, up to six samples (one using each barcode) are pooled together and purified. In the sequencing results, the specific samples are identified based on the sequence of the barcode. The NGS FASTQ files were shared with bioinformaticians at University of Missouri for analysis. For their analysis, they ran the FASTQ files through a computational code that sorts the sequences based on the presence of each barcode, and the sequence between the barcode and editing site. Any sequences that do not match the expected sequence are discarded. The remaining sequences are then sorted and counted to determine the number of sequences that have either an A or G nucleotide at the

specific editing location, per barcode. From these results, the percent G is reported, which is the same as the percent editing for this sequence. The error is also estimated by also reporting the number of non-A or non-G nucleotides at the edited position.

Table 4. PCR primers for NGS

Target	oRU #	Barcode	Primer Sequence with barcode
FLNB	120	GAGAG	GAGAGGAGTTCAGCATCTGGACCCG
FLNB	121	TTCTT	TTCTTGAGTTCAGCATCTGGACCCG
FLNB	122	CCTCC	CCTCCGAGTTCAGCATCTGGACCCG
FLNB	123	ACGCA	ACGCAGAGTTCAGCATCTGGACCCG
FLNB	124	CGTGC	CGTGCGAGTTCAGCATCTGGACCCG
FLNB	125	TACAT	TACATGAGTTCAGCATCTGGACCCG
CAPS1	103	GAGAG	GAGAGTGGCCGACGCCTACGTGACT
CAPS1	104	TTCTT	TTCTTTGGCCGACGCCTACGTGACT
CAPS1	105	CCTCC	CCTCCTGGCCGACGCCTACGTGACT
CAPS1	106	ACGCA	ACGCATGGCCGACGCCTACGTGACT
CAPS1	107	CGTGC	CGTGCTGGCCGACGCCTACGTGACT
CAPS1	108	TACAT	TACATTGGCCGACGCCTACGTGACT
FLNB	128	GAGAG	GAGAGCTCTCCCCTTTCGCACCATTCAACC
FLNB	129	TTCTT	TTCTTCTCTCCCCTTTCGCACCATTCAACC
FLNB	130	CCTCC	CCTCCCTCTCCCCTTTCGCACCATTCAACC
FLNB	131	ACGCA	ACGCACTCTCCCCTTTCGCACCATTCAACC
FLNB	132	CGTGC	CGTGCCTCTCCCCTTTCGCACCATTCAACC
FLNB	133	TACAT	TACATCTCTCCCCTTTCGCACCATTCAACC

RESULTS

The research goal was to determine if RNA editing changes during inflammation in a tissue and/or sex-specific manner. Inflammation was induced by injecting mice with 15 mg/kg body weight of 1 mg/mL LPS. Four hours after injection, tissues, including the heart, brain and skeletal muscle were harvested. Previous studies have found that the highest expression of ADAR1 was four hours after a similar dose of LPS. The same research found that inflammatory cytokines such as IFN-y were also highest between 2-4 hours after LPS injection (Kabir *et al*, 2002) A parallel project in the Ulbricht lab (M.S. student Christian Rivas) verified this LPS dose and timing resulted in systemic inflammation in these mice. RNA editing of four targets was quantified from dissected tissue from LPS treated mice, or co-housed littermate control mice treated with saline (Figure 8). The targets are edited by different enzymes, expressed in both the heart and brain, and previously shown to have tissue-specific editing rates (Ulbricht *et al*, 2017; Czermak *et al,* 2018; Shallev *et al,* 2018). The four targets tested are *FLNA*, *FLNB*, *CAPS1* and *Gria2*.

To determine the rate of RNA editing, the region surrounding the RNA editing site is amplified by RT-PCR and the amplicons are sequenced. An edited nucleotide will appear as a G instead of the genomically encoded A at that position. Editing rate is calculated by the percent G at the edited position.

Confirmation of RT-PCR Products

RT-PCR was used to amplify the edited region of RNA editing targets *FLNA*, *FLNB*, *CAPS1*, or *Gria2*. To optimize primers, PCR was performed on the same cDNA with increasing

annealing temperatures. The goal was to find the highest melting temperature (Tm) that gave the

most robust product with as minimal background product as possible (Figure 9). RT-PCR

products were visualized by agarose gel electrophoresis with ethidium bromide staining (Figure

9). The gradient PCR was performed for each new set of primers. The first *FLNA* primers used,

oRU 44 and 45, had a product size of 546 base pairs, and the most robust product at 54 ºC.

Therefore, the annealing temperature of 54 ºC was selected for amplification of *FLNA* with oRU

44 and 45 (Figure 9A). The Sanger sequencing of this PCR product lacked distinct peaks around

the editing site, preventing an accurate estimation of editing rates. New primers for *FLNA* were

developed: oRU 101 and 102 (Figure 9B). The product size for this primer set was 249 base

pairs. The best product with the least amount of background product was found at 60 ºC,

therefore, this was the annealing temperature selected for amplification of *FLNA* with these

primers.
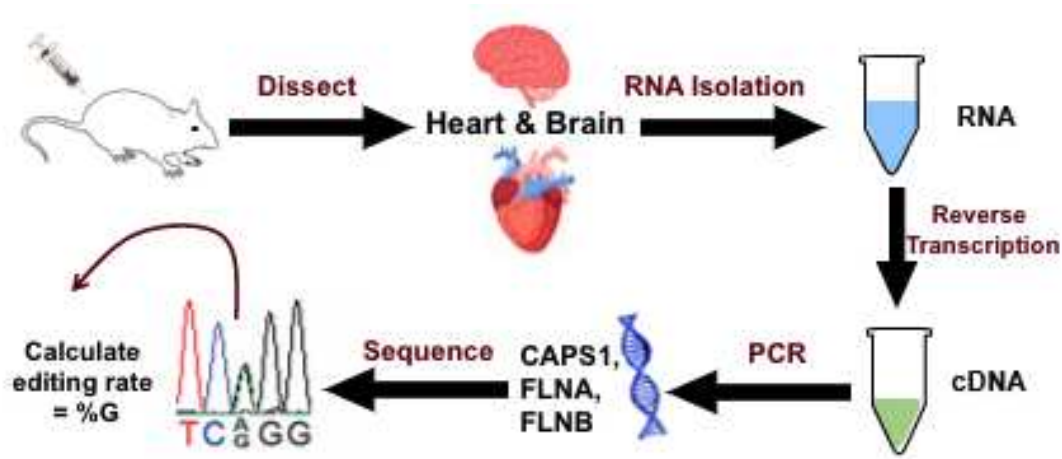
Figure 8. Methods overview. Wild type C57/Bl6 mice are injected with LPS or saline between 10-12 weeks of age. Four hours after injection, organs including the heart, brain, and skeletal muscle are harvested. RNA is isolated from the whole organs and then reverse transcribed into cDNA. cDNA is used as a template in PCR reactions for targets *CAPS1*, *FLNA*, and *FLNB*. DNA is purified from the PCR products and sent for sequencing to determine the percent editing in each target.

The next target for primer optimization was *FLNB*. The primers used were oRU 116 and 117. The annealing temperature selected for this target was 60 ºC due to the most robust product (Figure 9C). The last two sets of primers to optimize were for the target *Gria2*. The first set of primers used was oRU 118 and 119. The optimal product and annealing temperature for these primers was 60 ºC with a product size of around 300 base pairs (Figure 9D). The second set of primers designed and optimized for *Gria2* was oRU 118 and 126. These primers gave a product size of around 330 base pairs, and the annealing temperature selected was 58 ºC (Figure 9E).

RT-PCR products from *FLNA, FLNB* and *CAPS1* editing targets were all initially sequenced by Sanger sequencing. The sequencing produces a trace of nucleotides with one peak for each nucleotide (Figure 10, 11A, 12A, 13). The edited location will have a characteristic double peak; one peak represents the genomically encoded A nucleotide, and a G peak represents the presence of A-to-I editing. To determine the percent editing, the area under each peak at the edited location is determined and the percent G, or percent editing, is calculated using the formula G/(A+G) x 100%.

The presence of genomic DNA or other contaminating DNA products may alter the appearance of the editing rate in that sample. Therefore, RT-PCR controls are essential. Negative controls include amplification from RT reactions lacking reverse transcriptase and also a PCR reaction that lacks cDNA. The lack of a corresponding piece of DNA on the agarose gel confirms that the products are due to amplification from the sample and not cross-contamination of reagents or from genomic DNA. Once a clean and uncontaminated product was verified, this PCR product was purified and subjected to sequencing. For example, in Figure 9B, C and E we see that *FLNA*, *FLNB* and *Gria2*, respectively, are amplified. There are significant products of the expected size in the experimental samples, but negative controls either lack product all

together or lack a product in a similar size range to the expected product. If there are no apparent

background products in a sample, for example in 9C, the product can be directly purified from

the PCR sample. However, the presence of significant other products in the lane, such as in 8B

and E, indicates that the desired product must be cut from the gel and purified to be used in
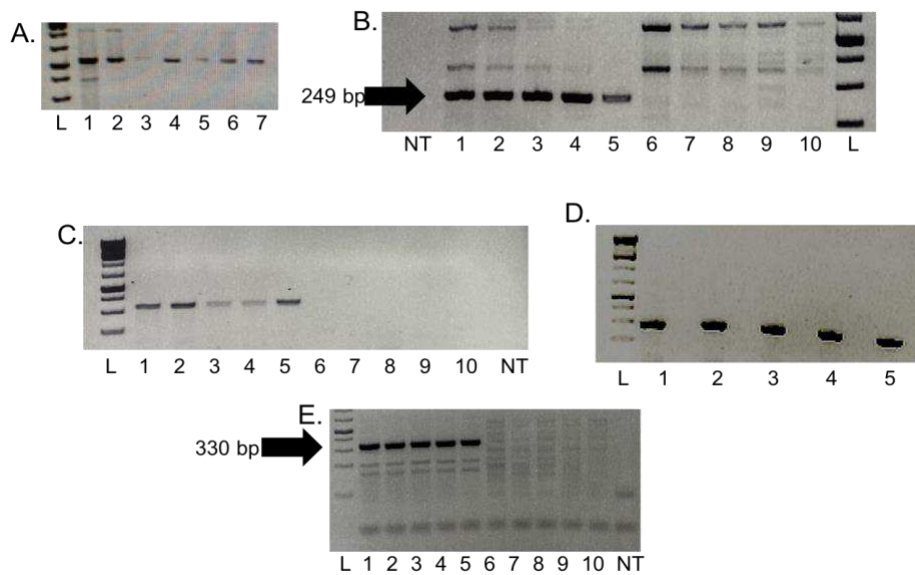
sequencing.

Figure 9. Primer optimization for editing targets. A-E. RT-PCR was performed and the products were analyzed by agarose gel electrophoresis. In each gel, the lane designated "L" is the ladder and "NT" is the non-template control. (A) Primers oRU 44 and 45 were used to amplify *FLNA* with Tm ranging from 54°C (lane 1) to 62°C (lane 7). The expected size from these primers is 546 base pairs. Lanes 1-7 contain the PCR product for *FLNA*. (B) Primers oRU 101 and 102 used to amplify *FLNA* with Tm ranging from 54.4°C (lane 1) to 60°C (lane 5). The expected product from these primers is 249 base pairs. Lanes 1-5 contain the PCR product for *FLNA*. The lanes 6-10 contain the controls, lacking reverse transcriptase (-RT). (C) Amplification of *FLNB* with primers oRU 116 and 117 with Tm ranging from 53°C (lane 1) to 60°C (lane 5). The expected product from these primers, seen in lanes 1-5, is 330 base pairs. Lanes 6-10 contain the -RT controls. (D) *Gria2* amplification with primers oRU 118 and 119 with Tm ranging from 53°C (lane 1) to 60°C (lane 5). Lanes 1-5 contain the PCR product for *Gria2*. (E) *Gria2* amplification with primers oRU 118 and 126 with Tm ranging from 52°C (lane 1) to 57.6°C (lane 5). The size of the expected *Gria2* product is ~330 base pairs. Lanes 1-5 are amplified from cDNA and lanes 6-10 contain products of -RT controls.
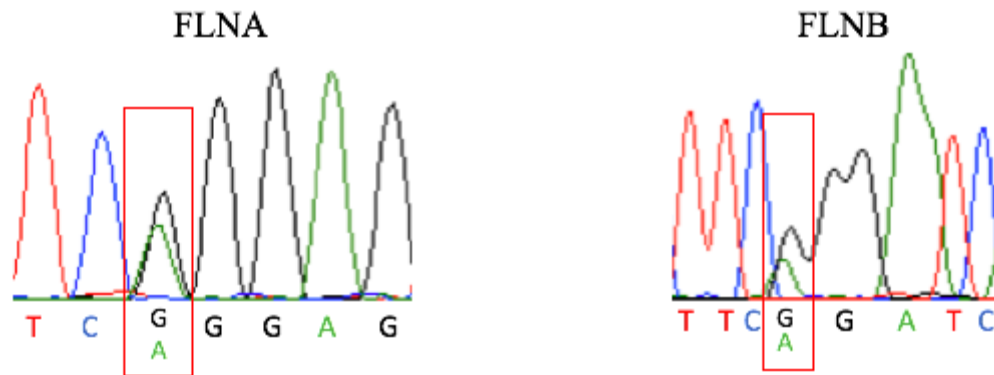
Figure 10. Representative chromatograms for *FLNA* and *FLNB*. Representative chromatograms for the edited region of *FLNA* (left) and *FLNB* (right). The edited location is highlighted by the red box.

Analysis of *FLNA* RNA Editing in the Heart and Brain

FLNA RNA editing was determined from Sanger sequencing chromatograms (Figure 11A, 12A). This location is identified by the double peak, indicating that editing is incomplete. There were eight mice in each of the four groups for analysis: female LPS, female saline, male LPS, and male saline. Each sample was sequenced at least twice. In the heart, the average editing for the female LPS group was 55%, the female saline group was 54%, the male LPS group was 59%, and the male saline group was 60% (2-way ANOVA, p-value for treatment groups = 0.9041, p-value for the sexes = 0.6898, Figure 11B). This indicates that there are no significant differences in *FLNA* editing between groups in the heart. There were also no significant differences between samples for *FLNA* editing in the brain, which had an average editing for the female LPS group of 41%, the female saline group was 42%, the male LPS group was 38%, and the male saline group was 41% (2-way ANOVA, p-value for treatment groups = 0.3683, p-value for the sexes = 0.2818, Figure 12B).

Co-housed littermates were paired and injected with LPS or saline, allowing us to compare the editing between each pair. The difference in *FLNA* editing between each LPS and

saline animal in each pair was calculated. In the heart, there was no significant difference in the change in editing when comparing males and females (t-test, p = 0.7995). In the brain, there was also no significant difference in the change in editing when comparing males and females (t-test, p = 0.2903, Figure 12C). This indicates that there was no difference in the way the heart and brain in males and females regulated RNA editing during inflammation.

Analysis of *Gria2* RNA Editing in the Brain

RNA editing of the target *Gria2* was also determined by Sanger sequencing following the same method used for *FLNA*. *Gria2* is neuron specific and normally 100% edited. If the editing of this target is disabled, the neuron will die. *Gria2* editing was analyzed in the brain of the saline and LPS injected mice to confirm long-term neuronal damage was not being induced in the inflammatory model. There were four mice in each group for analysis. In all groups, female LPS, female saline, male LPS, and male saline, the editing at the specific nucleotide was 100% (Figure 13). Therefore, the induced inflammation via LPS did not downregulate the editing of *Gria2* and therefore did not cause irreversible neuronal damage.

Analysis of *FLNB* RNA Editing in the Heart and Brain

FLNB RNA editing was determined by next generation sequencing (NGS). The Sanger sequencing results for *FLNB* were inconclusive due to the editing location not forming a complete peak on the chromatogram, making it impossible to accurately measure the area under the peak (Figure 10). For NGS, *FLNB* RT-PCR samples with barcoded primers were multiplexed into eight groups: male LPS, male saline, female LPS, and female saline for the heart and male LPS, male saline, female LPS, and female saline for the brain. When the NGS was performed,

the average editing of each pooled sample was reported. After NGS, the pooled samples may by de-multiplexed with a computational code to determine the editing of each individual mouse based on the barcode associated with that sample, however, the de-multiplexing was not completed in time to be included in this thesis. The average editing in the heart for the male LPS group was 66.4% and 64.3%, the male saline group was 65.7% and 58.2%, the female LPS group was 62.2%, and the female saline group was 65.5%. This reveals no significant difference in editing for the males and females between treatment groups (2-way ANOVA, p-value for treatment groups = 0.9895, p-value for the sexes = 0.9581, Figure 14A). There was also no significant difference in editing for males and females between treatment groups in the brain. The male LPS group had an average editing of 35.2% and 34.1%, the male saline group had an average editing of 33.1% and 33.9%, the female LPS group had an average editing of 35.1% and 65.3%, and the female saline group had an average editing of 36.3%, 34.5%, and 35.9% (2-way ANOVA, p-value for treatment = 0.2779, p-value for the sexes = 0.2324, Figure 14B).

Analysis of *CAPS1* RNA Editing in the Heart and Brain

CAPS1 was also analyzed using NGS. There is little expression of *CAPS1* in the heart, therefore the RT-PCR products for heart were nearly undetectable (Figure 15). However, *CAPS1* is robustly expressed in the brain. *CAPS1* amplification products from the heart were combined with at least one brain sample before purification to provide a significant, detectable DNA concentration necessary for sequencing preparation. These reads from the multiplexed samples were also sorted and counted to determine the percent editing of each individual mouse sample. Our results show no significant difference in editing between treatment groups in the heart and brain (1-way ANOVA, p-value = 0.1186, Figure 16).

Figure 11. RNA editing of *FLNA* in the heart of male and female mice. (A) Representative chromatograms of sequencing of RT-PCR amplicons from *FLNA*. The average editing for each group (female/male, LPS/saline) was calculated and the corresponding editing is displayed below the editing site. (B) Average percent editing of *FLNA* in the hearts of males and females in both treatment groups. *ANOVA,* $p_{treatment} > 0.05$ (n.s.), $p_{sex} > 0.05$ (n.s.). (C) The change in editing in the heart between LPS and saline treated co-housed littermate pairs. *T-test,* $p > 0.05$ (n.s.). Error bars (B, C) indicate the standard error of the mean (SEM). (n = 32; technical replicates ≥ 2).
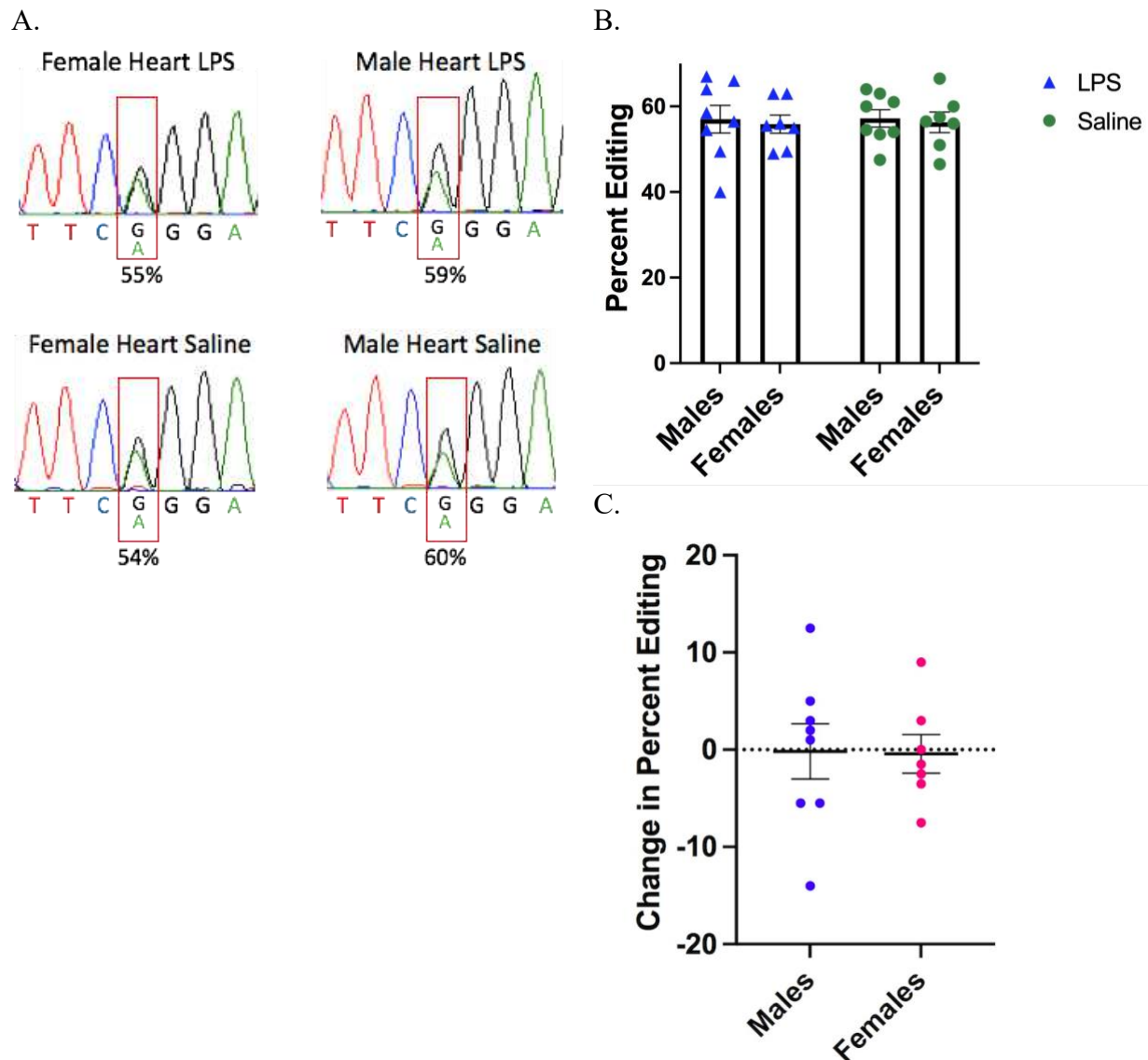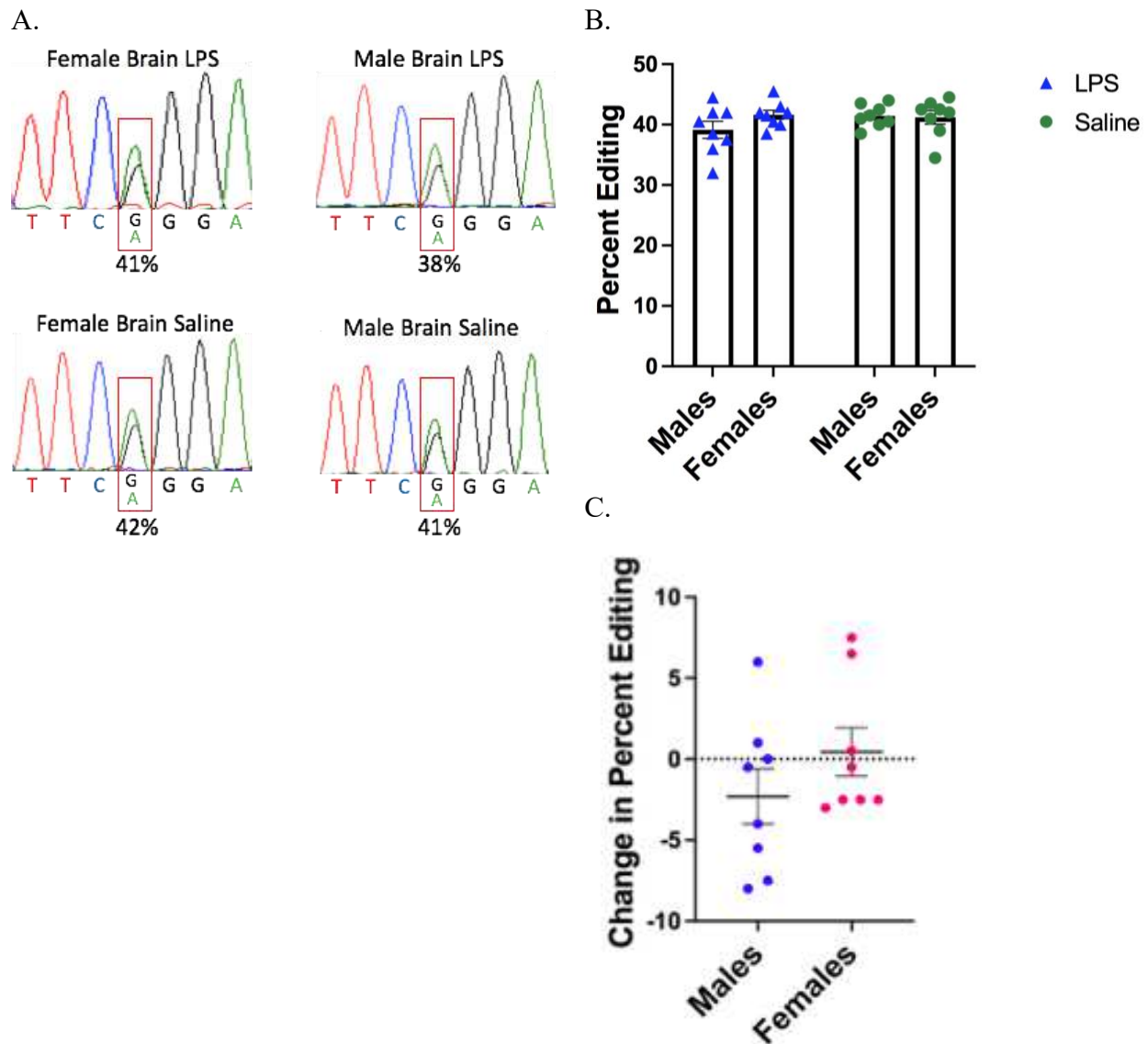
Figure 12. RNA editing of *FLNA* in the brain of male and female mice. (A) Representative chromatograms of sequencing of RT-PCR amplicons from *FLNA.* The average editing for each group (female/male, LPS/saline) was calculated and the corresponding editing is displayed below the editing site. (B) Average percent editing of *FLNA* in the brains of males and females in both treatment groups. *ANOVA,* $p_{treatment} > 0.05$ (n.s.), $p_{sex} > 0.05$ (n.s.). (C) The change in editing in the brain between LPS and saline treated co-housed littermate pairs. *T-test,* $p > 0.05$ (n.s.). Error bars (B, C) indicate the standard error of the mean (SEM). (n = 32; technical replicates $\geq$ 2)
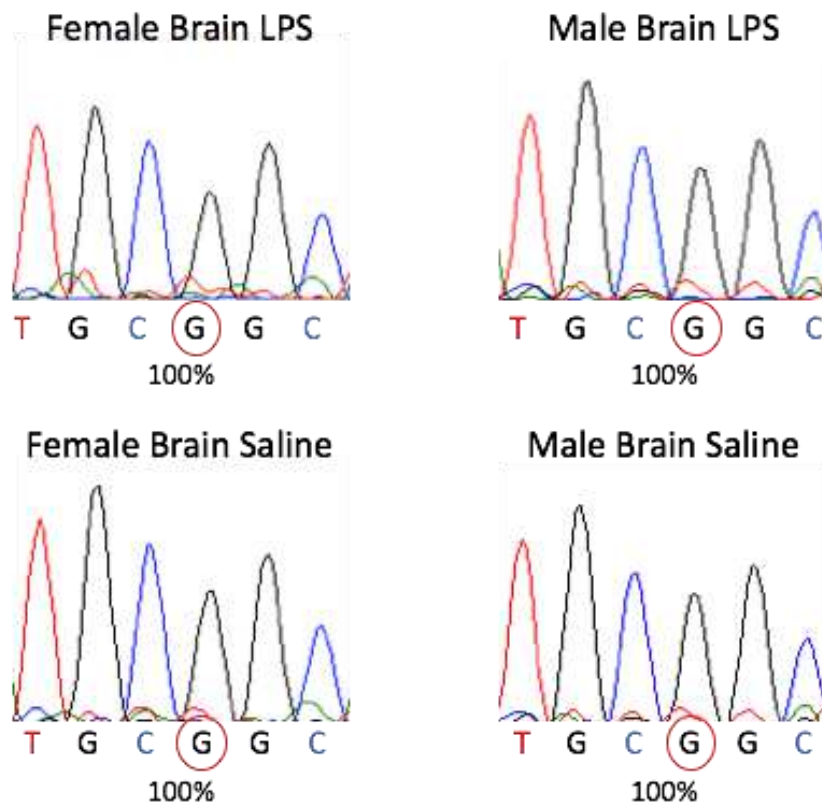
Figure 13. RNA editing of *Gria2* in the brain. Representative chromatograms from Sanger sequencing of *Gria2* RT-PCR amplicons from brains of female mice injected with LPS, female mice injected with saline, male mice injected with LPS, or male mice injected with saline. The edited nucleotide circled in red. The percent editing from each individual chromatogram is shown below the edited nucleotide.

Preliminary Results for Aim 2: Analysis of *FLNA* RNA Editing in Skeletal Muscle

To continue observing editing patterns in various tissues, the editing of *FLNA* was

analyzed in skeletal muscle. *FLNA* and *FLNB* are both expressed similarly in skeletal muscle,

however FLNB has a more important role in skeletal muscle while FLNA has a more important

role in cardiovascular tissue (Czermak *et al,* 2018; Jain *et al*, 2018). The same four groups as

previously described were used for the skeletal muscle samples. FLNA RNA editing was

determined from twelve mice in this preliminary study: three co-housed littermate pairs (LPS

and saline treated) for females and 3 co-housed littermate pairs for males. Skeletal muscle from

the abdominal wall was isolated, RNA was extracted, and reverse transcription performed to make cDNA. PCR was performed using the fresh cDNA and the samples were purified and prepared for Sanger sequencing. The average editing for the female LPS group was 33%, the female saline group was 39%, the male LPS group was 44%, and the male saline group was 47% (Figure 17). With the limited sample number, there is a significant difference between the editing in males and females as well as a difference between each treatment group (2-way ANOVA, p-value for the treatment = 0.0335, p-value for the sexes = 0.0187, Figure 17). Therefore, *FLNA* editing is dependent upon sex and appears to be influenced by inflammation in both males and females. However, data showing the change in editing between co-housed littermate pairs in skeletal muscle for males and females shows no difference in the change between LPS and saline (t-test, $p > 0.999$, Figure 17C). This indicates that while editing is sex-dependent, the inflammation induced editing is not sex-specific. Since there was a change in editing of *FLNA* in skeletal muscle but not in the heart, a correlation was performed to determine if the editing in either tissue was dependent on the other (Figure 18). No correlation was found ($R^2 = 0.3006$), indicating that the editing in different tissues is independent of one another.

A.   B.
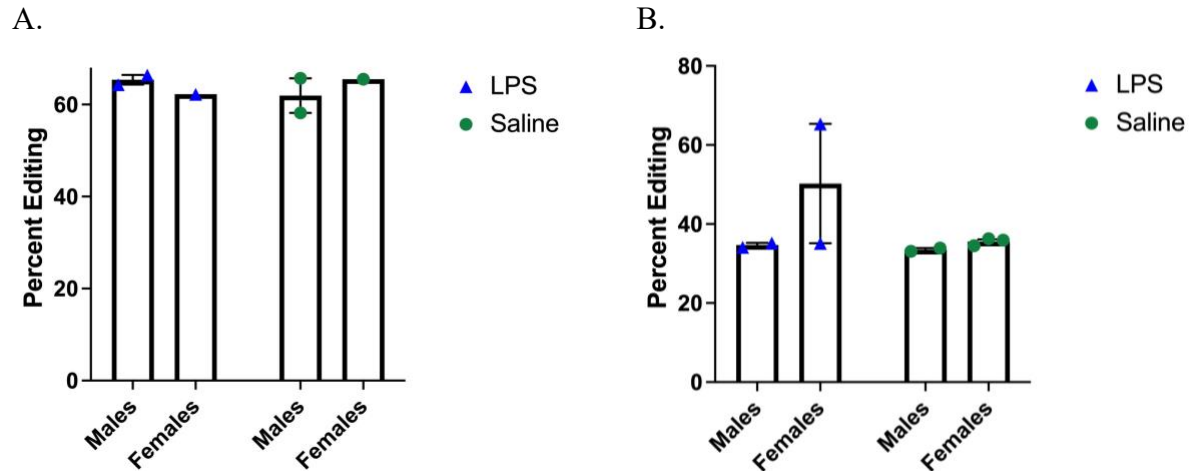
Figure 14. RNA editing of *FLNB* in the heart and brain. RNA editing of *FLNB* in the heart and brain was quantified through NGS. *FLNB* RT-PCR amplicons from each group (LPS treated males, saline treated males, LPS treated females, saline treated females) were pooled and subjected to NGS (n > 2). Average editing reported as the percent of G nucleotides that were present in the sequences. (A) *FLNB* editing in the heart. *ANOVA*, $p_{treatment} > 0.05$ (n.s.), $p_{sex} > 0.05$ (n.s.). (B) *FLNB* editing in the brain. *ANOVA*, $p_{treatment} > 0.05$ (n.s.), $p_{sex} > 0.05$ (n.s.) (n = 8).
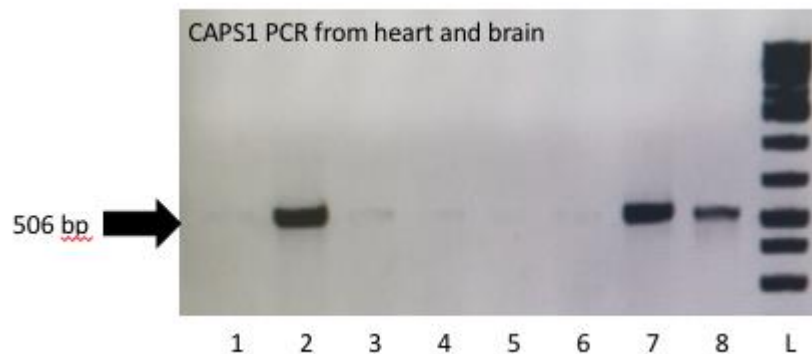
Figure 15. *CAPS1* amplification from the heart and brain. RT-PCR product was electrophoresed on an agarose gel to confirm amplification of *CAPS1*. Lanes 1-6 are RT-PCR products from heart and lanes 7-8 are RT-PCR products from brain samples. The last lane, designated "L", is the 1kb plus DNA ladder for comparison.
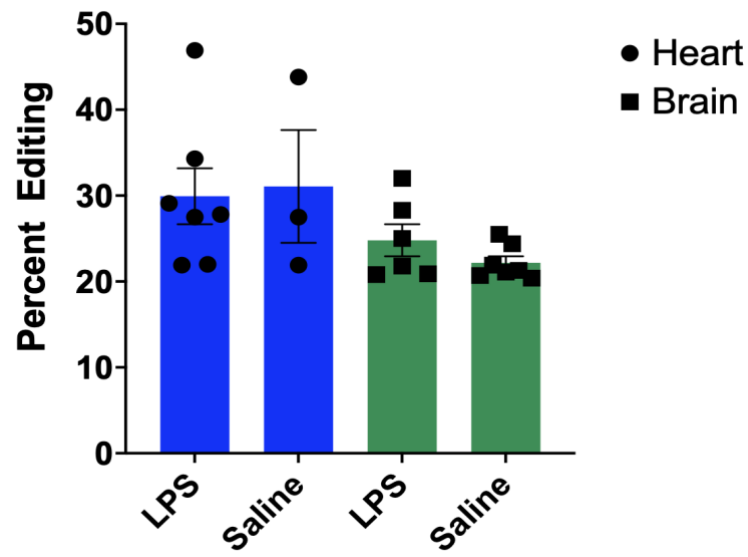
Figure 16. RNA editing of *CAPS1* in the heart and brain. RNA editing of *CAPS1* was quantified from the heart and brain of male and female mice by NGS. Percent editing from individual samples was calculated from the number of reads with G and A at the RNA editing site. *ANOVA*, p > 0.05 (n.s.). Error bars indicate the standard error of the mean (SEM). (n = 23)
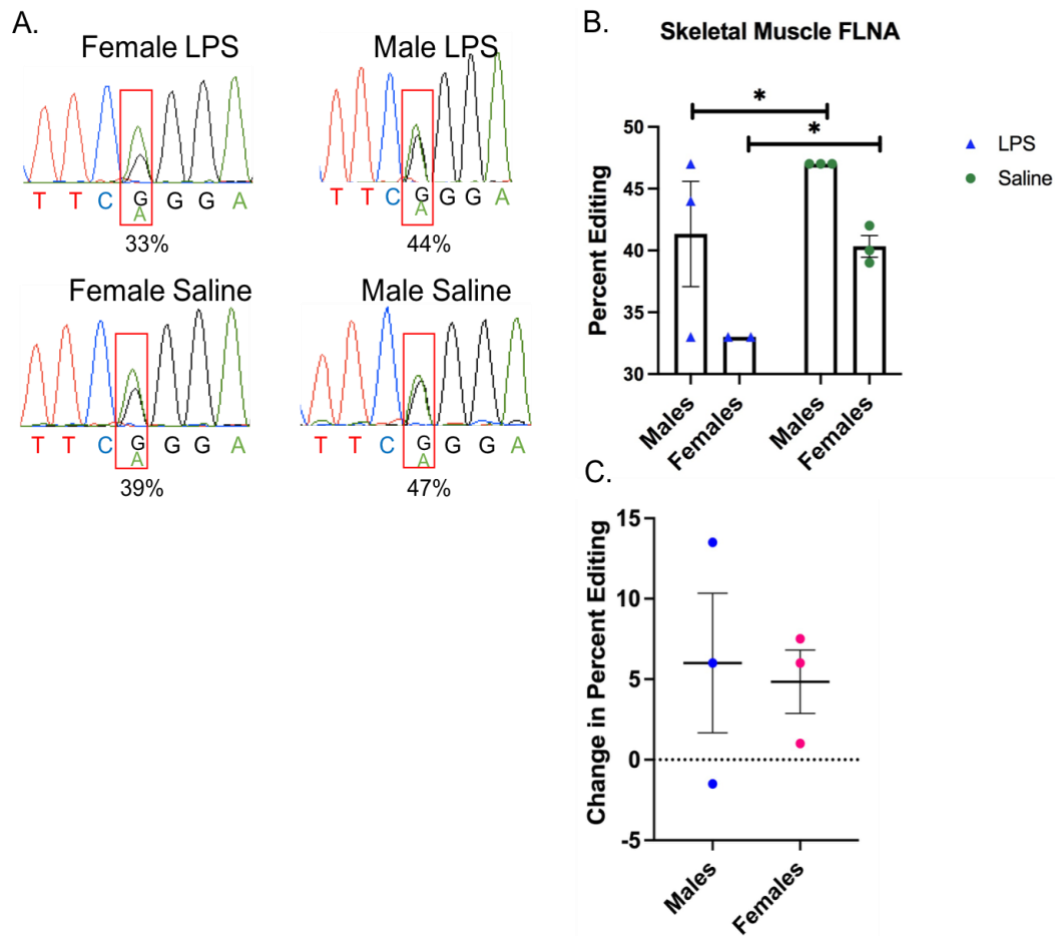
Figure 17. RNA editing of *FLNA* in skeletal muscle. (A) Representative chromatograms of sequencing of RT-PCR amplicons from *FLNA*. The average editing for each group (female/male, LPS/saline) was calculated and the corresponding editing is displayed below the editing site. (B) Average percent editing of *FLNA* in the skeletal muscle of males and females in both treatment groups. *ANOVA*, $p_{treatment} = 0.0335$ (significant), $p_{sex} = 0.0187$ (significant). (C) The change in editing in the skeletal muscle between LPS and saline treated co-housed littermate pairs. *T-test,* $p > 0.05$ (n.s.). Error bars (B, C) indicate the standard error of the mean (SEM). (N = 3, n = 12).
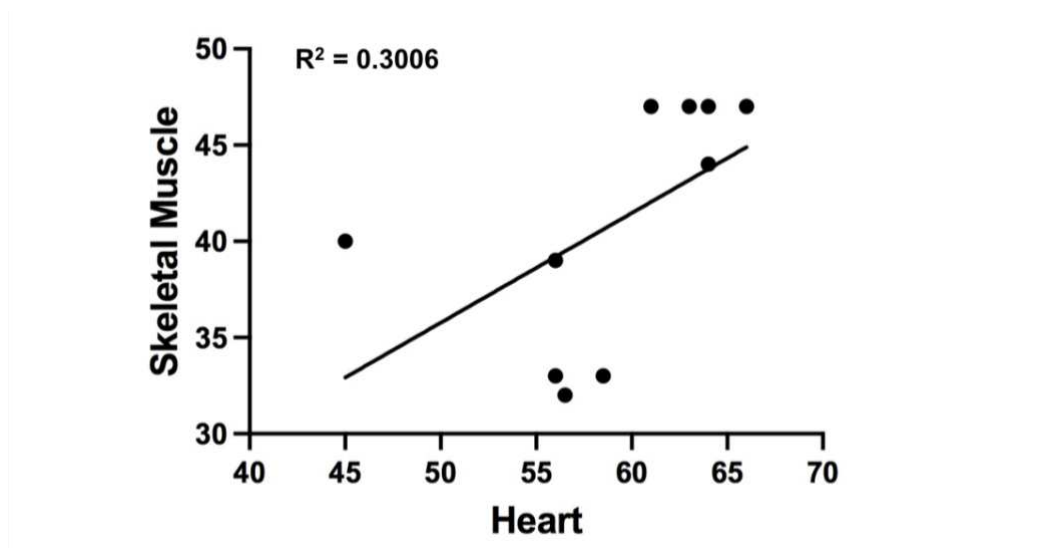
Figure 18. Correlation between *FLNA* editing in heart and skeletal muscle during inflammation. Editing of *FLNA* in the heart and skeletal muscle samples were compared. Both LPS and saline injected samples were used for comparison (n = 10). R^2 = 0.3006 (no correlation).

DISCUSSION

The goal of this research was to determine if inflammation alters RNA editing in a tissue specific and/or sex-specific manner. LPS was used to induce inflammation, and therefore, also induce ADAR1 p150 expression. ADAR1 regulation is vital in order for regulation of innate immunity, but RNA editing is also an important regulator of physiology in the body. Knowledge of if, or how, editing correlates with levels of ADAR1 will help us better understand the effects of inflammation and also how to combat unwanted effects of innate immunity related to ADAR1 p150. Additionally, this is the first study, to our knowledge, that comprehensively examines RNA editing in both males and females. Previous studies are either performed exclusively on male animals or only include female animals in overall analysis. Research that separately analyzes RNA editing in females is important to help understand if RNA editing may contribute to the sex-differences in inflammation and related health disparities.

Inflammatory Models

In the current model, the dose and timing of LPS injection is expected to show a maximal, acute innate immune reaction. The LPS injected mice were visibly sick at the time of dissection. They appeared lethargic and less responsive compared to the saline treated mice that were active within the cage and vigorously avoided being picked up. Therefore, it is likely that LPS indeed conferred significant activation of innate immunity. Quantification of ADAR1 p150 induction and other ISGs like TNF-alpha from the heart and brain is not included in this thesis but is being performed in parallel. Quantitative reverse transcription PCR (qRT-PCR) was performed on 14 of the mice (seven saline treated and LPS treated pairs). All mice had

upregulation of TNF-alpha in the heart, as expected, but the induction of ADAR1 p150 in the heart was less consistent (data now shown, C. Rivas & K. Kendrick). However, semi-quantitative RT-PCR showed consistent upregulation of ADAR1 p150 in skeletal muscle of LPS treated mice (data not shown, R. Ulbricht). The rest of the mice, as well as additional tissues, will need to be analyzed for the expression of ADAR1 p150 and TNF-alpha in order to confirm that inflammation was induced in the LPS injected mice and that all tissues responded to the inflammation.

While ADAR1 p150 levels are shown to peak at this time and dose of LPS (Kabir *et al*, 2002), it is possible that the activity of ADAR1 p150 is delayed, thus there is no effect on RNA editing of *FLNA*, *FLNB*, *Gria2*, or *CAPS1* in the heart and brain at this time. Therefore, investigating RNA editing and ADAR1 p150 levels at later time points could affect the results. This could be done by injecting with LPS and then harvesting tissues 6-12 hours later instead of 4 hours. While 4 hours post LPS injection had high levels of ADAR1 p150, there were still high levels of inflammatory markers several hours after that point (Kabir *et al,* 2002). Collecting tissues at these extended time points could help give a better picture of the inflammatory status after LPS injection.

It is also possible that the period of ADAR1 p150 induction after a single LPS injection is insufficient to induce significant changes, but that longer periods or repeated exposure to LPS may result in alterations to ADAR1 p150 activity that are sufficient to induce changes in RNA editing. Injecting a lower dose of LPS once a week for more than four weeks has been shown to induce more chronic inflammation (Kubera *et al*, 2013). This type of model might more closely mimic the viral infection in the preliminary data, but also mimic the types of chronic innate

immune activation shown to cause autoimmune disease and be associated with altered ADAR1 p150 levels in human disease.

Alternatively, a human disease model that includes sustained inflammation would provide a longer period of ADAR1 p150 induction and possibly provide opportunity for editing to be influenced. Chronic inflammation models like diet induced obesity, smoke exposure, or an autoimmune disease model like psoriasis (Shallev *et al*, 2018) have all been shown to have increased cytokine activity and/or induced ADAR1 p150. Changes in editing of *FLNA* and *FLNB* have been observed in the psoriasis model (Shallev *et al,* 2018), so investigating other common inflammatory conditions to observe possible changes in editing is warranted. Long term induction of ADAR1 p150 may promote long term changes in RNA editing, but also compensatory mechanisms may reduce ADAR1 editing activity to reduce unintended consequences of inflammation.

Tissue-Dependent RNA editing

The literature (Hood *et al*, 2014) and current evidence from the Ulbricht lab suggests that ADAR1 p150 induction is tissue-specific. Consistent upregulation of ADAR1 p150 in the skeletal muscle, but not in the heart or brain, might explain the tissue-specific effects that LPS has on RNA editing of *FLNA*. It would be worthwhile to continue investigating the editing levels in additional tissues during inflammation. For example, during normal conditions, there is high editing and expression of *FLNA* in tissues such as the stomach and small intestine (Jain *et al,* 2018). However, it is not known how this editing might change during inflammation. Also, considering the function of *CAPS1* is to regulate secretion, it could also be beneficial to look at

how the editing of this target could change in other secretory organs such as the pancreas or pituitary.

   RNA Editing in the Heart and Brain. Previous research (Ulbricht, unpublished) showed tissue specific changes in RNA editing of *CAPS1*, an ADAR1 target, in virus infected mouse pups. Editing in the heart was significantly increased, however editing in the brain was unaffected by viral infection (Hood *et al,* 2014). These results are inconsistent with those results and show that editing of *CAPS1* was unaffected in either heart or brain. *FLNA* RNA editing in the brain was not affected by the viral infection in previous studies (Hood *et al,* 2014), and also was not affected by LPS treatment in either brain or heart in our studies. *FLNB* RNA editing was also similar between LPS and saline treated mice in both the heart and brain. Based on the literature, we know RNA editing in different tissues varies. For example, *FLNA* editing in the heart and skeletal muscle is typically around 30% edited, while the editing in the brain is closer to 40% (Jain *et al,* 2018). However, our observations seem to differ from what is cited in the literature for the heart but are consistent with what we found in the brain. We found higher editing of *FLNA* in the heart and the same editing in the brain, around 40% (Figure 11, 12).

   Our studies (Figure 14), as well as previous studies (Hood *et al*, 2014) indicate that editing of the ADAR2 editing target, *Gria2*, remains consistent during inflammation. This restriction of *Gria2* RNA editing preserves neuronal function and may be a key reason why editing seems to be tightly regulated in the brain. If there is as little as a 10% decrease in editing of *Gria2*, the AMPA receptor becomes permeable to calcium, which causes neuronal death and neurological phenotypes such as ALS (Rosenthal, 2015). Perhaps evolution has installed tight regulation of RNA editing in order to maintain physiological integrity during conditions of stress or inflammation. This level of control restricts editing of the key target *Gria2*, as well as other

targets. A reduction in editing of *FLNA* during inflammation alters protein interactions with the target and could lead to vascular remodeling and hypertension (Jain *et al*, 2018). Increased editing of *FLNB* has been associated with several types of cancer, including hepatocellular carcinoma (Chan *et al*, 2014). Increasing the editing of *CAPS1* would increase the amount of release of vesicular contents into extracellular space (Miyake *et al,* 2016). No change in editing in the heart and brain during inflammation indicates a regulatory mechanism that maintains the levels of RNA editing during disrupted homeostasis, which is advantageous to the organism.

  RNA Editing in Skeletal Muscle. As part of the second aim for this research, RNA editing of *FLNA* and *FLNB* was quantified in skeletal muscle. This was done to continue investigating the possible tissue-dependent differences in RNA editing. Few publications have taken a detailed look at the editing in skeletal muscle, especially for *FLNA*. One study found almost no editing activity in skeletal muscle of cows (Bakhtiarizadeh *et al,* 2018), while another found editing activity for *FLNB* in mice (Czermak *et al,* 2018). In this study, there was a significant decrease in editing of *FLNA* in skeletal muscle with LPS treatment (Figure 17), which can be attributed to competitive inhibition of ADAR2 by ADAR1 during inflammation that is specific to skeletal muscle. While the number of mice included in this analysis is limited (n = 12) the results are statistically significant for both treatment and sex.

  The results of *FLNB* editing in skeletal muscle are not complete, but it will be interesting to compare the change in editing of another ADAR2 target to see if it follows a similar trend to *FLNA*. We can take the information we have from eliminating *FLNA* editing in the cardiovascular tissue and apply it to what could possibly happen in skeletal muscle. When *FLNA* editing is eliminated in the cardiovascular tissue, there is increased contractility due to mislocalization of signaling molecules for muscle contraction (Jain *et al,* 2018). We speculate

that the same type of response would occur in skeletal muscle. It is possible that this editing is not as regulated during inflammation because the possible side effects of downregulated editing in skeletal muscle are less severe than the effects in cardiovascular tissue and nervous tissue. While not much is known on the effects of reducing editing levels of *FLNB* in skeletal muscle, reduced expression of *FLNB* is associated with skeletal muscle atrophy (Turner *et al*, 2019). It is possible that reducing the editing of *FLNB* could cause similar side effects. While both cardiovascular remodeling and skeletal muscle atrophy can be reversed, muscle atrophy is less life threatening compared to the changes in cardiovascular tissue we see during elimination of *FLNA* editing (Jain *et al*, 2018).

Sex-Dependent RNA editing

The comprehensive editing profile from female mice is the first of its kind. To determine if there are sex-dependent effects of inflammation in males and females, RNA editing of *CAPS1*, *FLNA*, *FLNB*, and *Gria2* was quantified in males and females in the heart, brain, and skeletal muscle. In the heart and brain, the results showed no significant effects of inflammation for any of the targets (Figure 13, 14, 15, 16, 17). It is interesting to note, however, that for *FLNA*, editing in females seems to be less variable compared to males in the heart and brain (Figure 13C, 14C), perhaps indicating more regulation of editing in females. For each pair of mice (LPS treated and saline treated), we calculated the change in editing. Males had a wider range of change in editing for each pair compared to the female pairs. This points to possible differences in inflammation regulation. Since males have a more pro-inflammatory response, this might indicate a lack of regulation of ADAR1 p150 and RNA editing, leading to their wide range of RNA editing rates. In the skeletal muscle, *FLNA* editing is significantly reduced in females, compared to males, in

both LPS and saline treated mice (Figure 17). However, there is no significant difference between the change in editing in males and females (Figure 17C). This indicates that males and females have the same editing response during inflammation, but that editing levels are sex-dependent.

While we know males and females respond differently to inflammation, we do not know if there are different levels of ADAR1 p150 in males and females. If there are, this could potentially be one reason we see sex-differences in editing in skeletal muscle. Further experiments need to be performed to determine if increased expression of ADAR1 p150 in female mice is responsible for reduced editing by ADAR2 in the skeletal muscle of female mice.

Another important consideration is that *FLNA* is on the X chromosome. One study showed that the amount of substrate can regulate the rate of RNA editing (Czermak *et al*, 2018). If *FLNA* escapes X inactivation, we would expect to see higher expression of this target in females. If the absolute amount of editing of this target is fixed, having a higher expression of the target would lead to an overall lower percentage of editing. This could be one of the reasons we see decreased editing of *FLNA* in females in skeletal muscle. But it could also be that the absolute amount of *FLNA* editing that occurs in the heart is different between males and females, but that the increased expression of *FLNA* in females masks it. To determine if *FLNA* expression may play a role in regulating its editing level, qRT-PCR is being performed to compare the expression level of *FLNA* in males and females.

Further Investigation of Tissue and Sex-Dependent RNA Editing

Further steps to continue this research would be to finish homogenizing skeletal muscle samples, isolate RNA, and perform RT-PCR for *FLNA* and *FLNB* to gather more editing data in

skeletal muscle and compare it to the data in the heart and brain. So far, 12 mice (3 male pairs and 3 female pairs) have been analyzed for skeletal muscle. There are still 20 mice left for analysis, 5 male pairs and 5 female pairs. Along with comparing skeletal muscle data to the data from the heart and brain, I would also try to correlate ADAR1 p150 expression in these tissues with the RNA editing in the tissues. Such a correlation would help to link the amount of ADAR1 p150 with the amount of editing. Another possible step would be to quantify the expression of other sex-dependent inflammatory markers such as MDA5. This would be valuable since ADAR1 p150 inhibits the function of MDA5, but MDA5 levels are higher in the heart of female mice (Koenig *et al*, 2014). If ADAR1 p150 levels correlate with MDA5, then one might assume that MDA5 activity maintains significant regulation during inflammation. However, if ADAR1 p150 levels are not also increased in female mice, this might mean that the dsRNA sensor could be activated and induce an inflammatory response, even in the absence of a stimulus (Guo *et al*, 2021; Liddicoat *et al*, 2015).

The information in this thesis is valuable in further understanding how the sexes respond to inflammation. Knowing that the editing response to inflammation in females is similar to males allows for generalization of previous studies across sexes. Scientific research often omits female subjects from studies, often using the excuse that hormone fluctuations in female mice will influence results of the study. This omission has the potential to contribute to sex-disparities in health and treatment options for human patients. Our study observed the same responses in males and females, while making no attempt to control for phases of the estra cycle, supporting the notion that hormone cycles in females do not influence all molecular processes. Our study would argue that including females in molecular research, particularly RNA editing research, could increase the power of studies.

It is also important to consider the differences in how organs will respond to inflammation in a manner that is independent of one another. It is shown in the literature that RNA editing is tissue dependent, but the different functions of each organ could be influenced differently by the editing of each target. Expanding this research into a chronic inflammatory model will continue to inform us of the consequences of innate immune activation and short-term infection versus long term infections and autoimmune diseases. For example, a virus infection such as COVID-19 causes global inflammation, which we now know could cause changes in RNA editing in some tissues. If these changes in editing lead to some of the side effects seen during infection, it could help lead to specific treatments for the affected organs. Another example is using interferon treatment as a therapy for certain cancers and infections such as HCV, HBV, and Kaposi Sarcoma. This treatment causes global inflammation and upregulation of ADAR1 (Li *et al*, 2021). The side effects of this treatment can be detrimental to the individual receiving it, but if we know the reason behind some of the side effects, that will lead to treating the individual side effects to help minimize the pain felt during treatment. This knowledge will help in understanding how to address global inflammation in a tissue and sex-specific manner.

REFERENCES

Akira S, K Takeda (2004) Toll-like receptor signaling. *Nat. Rev. Immunol* 4: 499–511

Bachmann MF, Kopf M (2001) On the role of the innate immunity in autoimmune disease. *The Journal of Experimental Medicine*

Bakhtiarizadeh Mohammad Reza, Salehi Abdolreza, Melissa Rivera Rocío (2018) Genome-wide identification and analysis of A-to-I RNA editing events in bovine by transcriptome sequencing. *PloS One* 13

Bandaru S, Ala C, Zhou A, Akyurek L (2021) Filamin A regulates cardiovascular remodeling. *Int J Mol Sci* 22: 6555

Ben-Shoshan Shirley Oren, Kagan Polina, Sultan Maya, Barabash Zohar, Dor Chen, Jacob-Hirsch Jasmine, Harmelin Alon, *et al* (2017) ADAR1 deletion induces NFκB and interferon signaling dependent liver inflammation and fibrosis. *RNA Biology* 14: 587–602

Cavasin Maria A, Zhen-Yin Tao, Ai-Li Yu, Xiao-Ping Yang (2006) Testosterone enhances early cardiac remodeling after myocardial infarction, causing rupture and degrading cardiac function. *American Journal of Physiology Heart and Circulatory Physiology* 290: 2043–2050

Chan Tim, Hon Man, Chi Ho Lin, Lihua Qi, Jing Fei, Yan Li, Kol Jia Yong, Ming Liu, *et al* (2014) A disrupted RNA editing balance mediated by ADARs (adenosine deaminases that act on RNA) in human hepatocellular carcinoma. *Gut* 63: 832–843

Cho Dan-Sung C, Weidong Yang, Lee Joshua T, Ramin Shiekhattar, Murray John M, Kazuko Nishikura (2003) Requirement of dimerization for RNA editing activity of adenosine deaminases acting on RNA. *The Journal of Biological Chemistry* 278: 17093–17102

Cooper Leslie T Jr (2009) Myocarditis. *The New England Journal of Medicine* 360: 1526–1538

Costa Cruz Pedro Henrique, Yuki Kato, Taisuke Nakahama, Toshiharu Shibuya, Yukio Kawahara (2020) A comparative analysis of ADAR mutant mice reveals site-specific regulation of RNA editing. *RNA* 26: 454–469

Czermak Philipp, Fabian Amman, Michael F Jantsch, Laura Cimatti (2018) Organ-wide profiling in mouse reveals high editing levels of Filamin B mRNA in the musculoskeletal system. *RNA Biology* 15: 877–885

Dawson Renee T, Christopher L Sansam, Ronald B Emeson (2004) Structure and sequence determinants required for the RNA editing of ADAR2 substrates. *The Journal Of Biological Chemistry* 279: 4941–4951

Feng Y, Chen M, Moskowitz I, Menonza A, Vidali L, Nakamura F, Kwiatkowski D, Walsh C (2006) Filamin A (FLNA) is required for cell-cell contact in vascular development and cardiac morphogenesis. *PNAS* 103: 19836-19841

Frisancho-Kiss Sylvia, Sarah E Davis, Jennifer F Nyland, J Augusto Frisancho, Daniela Cihakova, Masheka A Barrett, Noel R Rose, Delisa Fairweather (2007) Cutting edge: cross-regulation by TLR4 and T cell Ig mucin-3 determines sex differences in inflammatory heart disease. *Journal of Immunology* 178: 6710–6714

Fu Y, Zhao X, Li Z, Wei J, Tian Y (2016) Splicing variants of ADAR2 and ADAR2-mediated RNA editing in glioma. *Oncol Lett* 12: 788-792

Gélinas Jean-François, Guerline Clerzius, Eileen Shaw, Anne Gatignol (2011) Enhancement of replication of RNA viruses by ADAR1 via RNA editing and inhibition of RNA-activated protein kinase. *Journal of Virology* 85: 8460–8466

George CX, Samuel CE (1999) Human RNA-specific adenosine deaminase ADAR1 transcripts possess alternative exon 1 structures that initiate from different promoters, one constitutively active and the other interferon inducible. *Proceedings of the National Academy of Sciences of the United States of America* 96: 4621–4626

George Cyril X, Gokul Ramaswami, Jin Billy Li, Charles E Samuel (2016) Editing of cellular self-RNAs by adenosine deaminase ADAR1 suppresses innate immune stress responses. *The Journal of Biological Chemistry* 291: 6158–6168

Guo Xinfeng, Clayton A Wiley, Richard A Steinman, Yi Sheng, Beihong Ji, Junmei Wang, Liyong Zhang, *et al* (2021) Aicardi-Goutières Syndrome-associated mutation at ADAR1 gene locus activates innate immune response in mouse brain. *Journal of Neuroinflammation* 18: 169

Hart Alan W, Joanne E Morgan, Jürgen Schneider, Katrine West, Lisa McKie, Shoumo Bhattacharya, Ian J Jackson, Sally H Cross (2006) Cardiac malformations and midline skeletal defects in mice lacking Filamin A. *Human Molecular Genetics* 15: 2457–2467

Hartner Jochen C, Carl R Walkley, Jun Lu, Stuart H Orkin (2009) ADAR1 is essential for the maintenance of hematopoiesis and suppression of interferon signaling. *Nature Immunology* 10: 109–115

Herbert A, Rich A (2001) The role of binding domains for dsRNA and Z-DNA in the in vivo editing of minimal substrates by ADAR1. *Proceedings of the National Academy of Sciences of the United States of America* 98: 12132–12137

Hsieh Ya-Ching, Michael Frink, Bjoern M Thobe, Jun-Te Hsu, Mashkoor A Choudhry, Martin G Schwacha, Kirby I Bland, Irshad H Chaudry (2007) 17Beta-estradiol downregulates

kupffer cell TLR4-dependent p38 MAPK pathway and normalizes inflammatory cytokine production following trauma-hemorrhage. *Molecular Immunology* 44: 2165–2172

Hood Jennifer L, Michael V Morabito, Charles R Martinez 3rd, James A Gilbert, Elizabeth A Ferrick, Gregory D Ayers, James D Chappell, Terence S Dermody, Ronald B Emeson (2014) Reovirus-mediated induction of ADAR1 (p150) minimally alters RNA editing patterns in discrete brain regions. *Molecular and Cellular Neurosciences* 61: 97–109

Jain Mamta, Tomer D Mann, Maja Stulić, Shailaja P Rao, Andrijana Kirsch, Dieter Pullirsch, Xué Strobl, *et al* (2018) RNA editing of Filamin A pre-mRNA regulates vascular contraction and diastolic blood pressure. *The EMBO Journal* 37

Jelinek W, Darnell JE (1972) Double-stranded regions in heterogeneous nuclear RNA from hela cells. *Proceedings of the National Academy of Sciences of the United States of America* 69: 2537–2541

Kabir Koroush, Jean-Pierre Gelinas, Meihong Chen, Dongfen Chen, Dexin Zhang, Xiaoxing Luo, Jing-Hua Yang, Darryl Carter, Reuven Rabinovici (2002) Characterization of a murine model of endotoxin-induced acute lung injury. *Shock* 17: 300–303

Kawahara Yukio, Molly Megraw, Edward Kreider, Hisashi Iizasa, Louis Valente, Artemis G Hatzigeorgiou, Kazuko Nishikura (2008) Frequency and fate of microRNA editing in human brain. *Nucleic Acids Research* 36: 5270–5280

Kim Dennis DY, Thomas TY Kim, Thomas Walsh, Yoshifumi Kobayashi, Tara C Matise, Steven Buyske, Abram Gabriel (2004) Widespread RNA editing of embedded Alu elements in the human transcriptome. *Genome Research* 14: 1719–1725

Koenig Andreas, Adam Sateriale, Ralph C Budd, Sally A Huber, Iwona A Buskiewicz (2014) The role of sex differences in autophagy in the heart during coxsackievirus B3-induced myocarditis. *Journal of Cardiovascular Translational Research* 7: 182–191

Kubera Marta, Katarzyna Curzytek, Weronika Duda, Monika Leskiewicz, Agnieszka Basta-Kaim, Boguslawa Budziszewska, Adam Roman, *et al* (2013) A new animal model of (chronic) depression induced by repeated and intermittent lipopolysaccharide administration for 4 months. *Brain, Behavior, and Immunity* 31: 96–104

Kumar Suresh, Trilochan Mohapatra (2021) Deciphering epitranscriptome: modification of mRNA bases provides a new perspective for post-transcriptional regulation of gene expression. *Frontiers in Cell and Developmental Biology* 9: 628415

Kwak Shin, Yoshinori Nishimoto, Takenari Yamashita (2008) Newly identified ADAR-mediated A-to-I editing positions as a tool for ALS research. *RNA Biology* 5: 193–197

Levanon EY, Hallegger M, Kinar Y, Shemesh R, Djinovic-Carugo K, Rechavi G, Jantsch MF, Eisenberg E (2005) Evolutionarily conserved human targets of adenosine to inosine RNA editing. *Nucleic Acids Res* 33: 1162–1168

Li Tao, Xiaoshuang Yang, Wei Li, Jiaru Song, Zhuo Li, Xilin Zhu, Xiaopan Wu, Ying Liu (2021) ADAR1 stimulation by IFN-α downregulates the expression of MAVS via RNA editing to regulate the anti-HBV response. *Molecular Therapy: The Journal of the American Society of Gene Therapy* 29: 1335–1348

Liddicoat Brian J, Robert Piskol, Alistair M Chalk, Gokul Ramaswami, Miyoko Higuchi, Jochen C Hartner, Jin Billy Li, Peter H Seeburg, Carl R Walkley (2015) RNA editing by ADAR1 prevents MDA5 sensing of endogenous dsRNA as nonself. *Science* 349: 1115–1120

Liu Xuefang, Sugai Yin, Yulong Chen, Yaosong Wu, Wanchun Zheng, Haoran Dong, Yan Bai, *et al* (2018) LPS-induced proinflammatory cytokine expression in human airway epithelial cells and macrophages via NF-κB, STAT3 or AP-1 activation. *Molecular Medicine Reports* 17: 5484–5491

Loirand Gervaise, Patrice Guérin, Pierre Pacaud (2006) Rho kinases in cardiovascular physiology and pathophysiology. *Circulation Research* 98: 322–334

Marriott Ian, Bost Kenneth L, Huet-Hudson Yvette M (2006) Sexual dimorphism in expression of receptors for bacterial lipopolysaccharides in murine macrophages: A possible mechanism for gender-based differences in endotoxic shock susceptibility. *Journal of reproductive immunology* 71: 12-27

Matthews Melissa M, Justin M Thomas, Yuxuan Zheng, Kiet Tran, Kelly J Phelps, Anna I Scott, Jocelyn Havel, Andrew J Fisher, Peter A Beal (2016) Structures of human ADAR2 bound to dsRNA reveal base-flipping mechanism and basis for site selectivity. *Nature Structural & Molecular Biology* 23: 426–433

Medzikovic Lejla, Christine M Cunningham, Min Li, Marjan Amjedi, Jason Hong, Gregoire Ruffenach, Mansoureh Eghbali (2020) Sex differences underlying preexisting cardiovascular disease and cardiovascular injury in COVID-19. *Journal of Molecular and Cellular Cardiology* 148: 25–33

Miyake K, Ohta T, Nakayama H, *et al* (2016) CAPS1 RNA editing promotes dense core vesicle exocytosis. *Cell Rep* 17: 2004-2014

Nakahama Taisuke, Yuki Kato, Toshiharu Shibuya, Maal Inoue, Jung In Kim, Tuangtong Vongpipatana, Hiroyuki Todo, Yanfang Xing, Yukio Kawahara (2021) Mutations in the adenosine deaminase ADAR1 that prevent endogenous Z-RNA binding induce Aicardi-Goutières-Syndrome-like encephalopathy. *Immunity* 54: 1976–1988

Nakamura F, Osborn T, Hartemink C, Hartwig J, Stossel T (2007) Structural basis of Filamin A functions. *J Cell Biol* 179: 1011-1025

Nakamura Fumihiko, Thomas P Stossel, John H Hartwig (2011) The Filamins: organizers of cell structure and function. *Cell Adhesion & Migration* 5: 160–169

Nishikura Kazuko (2010) Functions and regulation of RNA editing by ADAR deaminases. *Annual Review of Biochemistry* 79: 321–349

Ota Hiromitsu, Masayuki Sakurai, Ravi Gupta, Louis Valente, Bjorn-Erik Wulff, Kentaro Ariyoshi, Hisashi Iizasa, Ramana V Davuluri, Kazuko Nishikura (2013) ADAR1 forms a complex with dicer to promote microRNA processing and RNA-induced gene silencing. *Cell* 153: 575–589

Pestal Kathleen, Cory C Funk, Jessica M Snyder, Nathan D Price, Piper M Treuting, Daniel B Stetson (2015) Isoforms of RNA-editing enzyme ADAR1 independently control nucleic acid sensor MDA5-driven autoimmunity and multi-organ development. *Immunity* 43: 933–944

Rueter S, Dawson T, Emeson R (1999) Regulation of alternative splicing by RNA editing. *Nature* 399: 75–80

Rice Gillian, Teresa Patrick, Rekha Parmar, Claire F Taylor, Alec Aeby, Jean Aicardi, Rafael Artuch, *et al* (2007) Clinical and molecular phenotype of Aicardi-Goutieres Syndrome. *American Journal of Human Genetics* 81: 713–725

Riedmann Eva M, Sandy Schopoff, Jochen C Hartner, Michael F Jantsch (2008) Specificity of ADAR-mediated RNA editing in newly identified targets. *RNA* 14: 1110–1118

Rosenthal Joshua JC (2015) The emerging role of RNA editing in plasticity. *The Journal of Experimental Biology* 218: 1812–1821

Scotland Ramona S, Melanie J Stables, Shimona Madalli, Peter Watson, Derek W Gilroy (2011) Sex differences in resident immune cell phenotype underlie more efficient acute inflammatory responses in female mice. *Blood* 118: 5918–5927

Seif Farhad, Majid Khoshmirsafa, Hossein Aazami, Monireh Mohsenzadegan, Gholamreza Sedighi, Mohammadali Bahar (2017) The role of JAK-STAT signaling pathway and its regulators in the fate of T helper cells. *Cell Communication and Signaling: CCS* 15: 23

Shallev Lea, Eli Kopel, Ariel Feiglin, Gil S Leichner, Dror Avni, Yechezkel Sidi, Eli Eisenberg, Aviv Barzilai, Erez Y Levanon, Shoshana Greenberger (2018) Decreased A-to-I RNA editing as a source of keratinocytes' dsRNA in psoriasis. *RNA* 24: 828–840

Sheen Volney L, Yuanyi Feng, Donna Graham, Toshiro Takafuta, Sandor S Shapiro, Christopher A Walsh (2002) Filamin A and Filamin B are co-expressed within neurons during periods of neuronal migration and can physically interact. *Human Molecular Genetics* 11: 2845–2854

Shi Y, ed (2017) Mrna Processing: Methods and Protocols. *New York: Human Press*

Shumate Kayla M, Sadik T Tas, Ege T Kavalali, Ronald B Emeson (2021) RNA editing-mediated regulation of calcium-dependent activator protein for secretion (CAPS1) localization and its impact on synaptic transmission. *Journal of Neurochemistry* 158: 182–196

Slotkin William, Kazuko Nishikura (2013) Adenosine-to-inosine RNA editing and human disease. *Genome Medicine* 5: 105

Spellberg B, JE Edwards Jr (2001) Type 1/Type 2 immunity in infectious diseases. *Clinical Infectious Diseases: An Official Publication of the Infectious Diseases Society of America* 32: 76–102

Stellos Konstantinos, Aikaterini Gatsiou, Kimon Stamatelopoulos, Ljubica Perisic Matic, David John, Federica Francesca Lunella, Nicolas Jaé, *et al* (2016) Adenosine-to-Inosine RNA editing controls cathepsin s expression in atherosclerosis by enabling HuR-mediated post-transcriptional regulation. *Nature Medicine* 22: 1140–1150

Stulić Maja, Michael F Jantsch (2013) Spatio-temporal profiling of Filamin A RNA-editing reveals ADAR preferences and high editing levels outside neuronal tissues. *RNA Biology* 10: 1611–1617

Tan Meng How, Qin Li, Raghuvaran Shanmugam, Robert Piskol, Jennefer Kohler, Amy N Young, Kaiwen Ivy Liu, *et al* (2017) Dynamic landscape and regulation of RNA editing in mammals. *Nature* 550: 249–254

Turner Daniel C, Robert A Seaborne, Adam P Sharples (2019) Comparative transcriptome and methylome analysis in human skeletal muscle anabolism, hypertrophy and epigenetic memory. *Scientific Reports* 9: 4251

Ulbricht Randi J, Sarah J Sun, Claire E DelBove, Kristina E Kitko, Saad C Rehman, Michelle Y Wang, Roman M Lazarenko, Qi Zhang, Ronald B Emeson (2017) RNA editing of CAPS1 regulates synaptic vesicle organization, release and retrieval. *bioRxiv*

Wang Guoliang, Hui Wang, Sucha Singh, Pei Zhou, Shengyong Yang, Yujuan Wang, Zhaowei Zhu, *et al* (2015) ADAR1 prevents liver injury from inflammation and suppresses interferon production in hepatocytes. *The American Journal of Pathology* 185: 3224–3237

Wang Yuru, Sehee Park, Peter A Beal (2018) Selective recognition of RNA substrates by ADAR deaminase domains. *Biochemistry* 57: 1640–1651

Wit Marie Claire Y de, Irenaeus FM de Coo, Maarten H Lequin, Dicky JJ Halley, Jolien W Roos-Hesselink, Grazia MS Mancini (2011) Combined cardiological and neurological

abnormalities due to Filamin A gene mutation. *Clinical Research in Cardiology: Official Journal of the German Cardiac Society* 100: 45–50

Yang Jing-Hua, Yongzhan Nie, Qingchuan Zhao, Yingjun Su, Marc Pypaert, Haili Su, Reuven Rabinovici (2003) Intracellular localization of differentially regulated RNA-specific adenosine deaminase isoforms in inflammation. *The Journal of Biological Chemistry* 278: 45833–45842

Zhang Jun-Ming, An Jianxiong (2007) Cytokines, inflammation, and pain. *International Anesthesiology Clinics* 45: 27–37

Zhang Xincai, Xiangting Gao, Jun Hu, Yuxin Xie, Yuanyi Zuo, Hongfei Xu, Shaohua Zhu (2019) ADAR1p150 forms a complex with dicer to promote miRNA-222 activity and regulate PTEN expression in CVB3-induced viral myocarditis. *International Journal of Molecular Sciences*

Zhou Alex-Xianghua, John H Hartwig, Levent M Akyürek (2010) Filamins in cell signaling, transcription and organ development. *Trends in Cell Biology* 20: 113–123

Zhou Xianghua, Fei Tian, Johan Sandzén, Renhai Cao, Emilie Flaberg, Laszlo Szekely, Yihai Cao, *et al* (2007) Filamin B deficiency in mice results in skeletal malformations and impaired microvascular development. *Proceedings of the National Academy of Sciences of the United States of America* 104: 3919–3924